T.C.
DOKUZ EYLUL UNIVERSITY
IZMIR INTERNATIONAL BIOMEDICINE
AND GENOME INSTITUTE

COMPARISON OF THE MOLECULAR MECHANISMS OF MELANOCYTE REGENERATION AND MELANOMA USING THE ZEBRAFISH

ESRA KATKAT

MOLECULAR BIOLOGY AND GENETICS

MASTER DISSERTATION

IZMIR-2018

2016850005

T.C.
DOKUZ EYLUL UNIVERSITY
IZMIR INTERNATIONAL BIOMEDICINE
AND GENOME INSTITUTE

COMPARISON OF THE MOLECULAR MECHANISMS OF MELANOCYTE REGENERATION AND MELANOMA USING THE ZEBRAFISH

MOLECULAR BIOLOGY AND GENETICS

MASTER DISSERTATION

ESRA KATKAT

Assoc. Prof. H. Güneş ÖZHAN

2016850005

T.C.

DOKUZ EYLÜL ÜNİVERSİTESİ
İZMİR ULUSLARARASI BİYOTIP VE GENOM ENSTİTÜSÜ MÜDÜRLÜĞÜ

YÜKSEK LİSANS TEZ ONAY FORMU

Dokuz Eylül Üniversitesi İzmir Uluslararası Biyotıp ve Genom Enstitüsü Genom Bilimleri ve Moleküler Biyoteknoloji Anabilim Dalı, Moleküler Biyoloji ve Genetik Yüksek Lisans Programı öğrencisi 2016850005 numaralı Esra KATKAT, **"COMPARISON OF THE MOLECULAR MECHANISMS OF MELANOCYTE REGENERATION AND MELANOMA USING THE ZEBRAFISH"** konulu Yüksek Lisans tezini 07.01.2019 tarihinde başarılı olarak tamamlamıştır.

BAŞKAN

Doç. Dr. H. Güneş ÖZHAN BAYKAN

DEÜ İzmir Uluslararası Biyotıp ve Genom Enstitüsü

Biyotıp ve Sağlık Teknolojileri Anabilim Dalı

JÜRİ ÜYESİ

Dr. Öğr. Üyesi Yavuz OKTAY

DEÜ Tıp Fakültesi

Temel Tıp Bilimleri Tıbbi Biyoloji Anabilim Dalı

JÜRİ ÜYESİ

Doç. Dr. Şerif ŞENTÜRK

DEÜ İzmir Uluslararası Biyotıp ve Genom Enstitüsü

Genom Bilimleri ve Moleküler Biyoteknoloji Anabilim Dalı

JÜRİ ÜYESİ

Doç. Dr. Özden YALÇIN ÖZUYSAL

İzmir Yüksek Teknoloji Enstitüsü Fen Fakültesi

Moleküler Biyoloji ve Genetik Bölümü

JÜRİ ÜYESİ

Prof. Dr. Şebnem AKTAN

DEÜ Tıp Fakültesi

Deri ve Zührevi Hastalıklar Anabilim Dalı

TABLE OF CONTENTS

LIST OF TABLES

LIST OF FIGURES

ABBREVIATIONS

4-HA : 4-Hydroxyamphetamin

CNS : Central Nervous System

DMSO : Dimethyl sulfoxide

dpa : day post ablation

dpf : day post fertilization

EGFP : Enhanced Green Fluorescent Protein

EMT : Epithelial to Mesenchymal Transition

MCSCs : Melanocyte stem cells

MOTP : Morpholinylbutylthio)phenol

NCCs : Neural Crest Cells

NCP : Neocuproine

NTR : Nitroreductase

PTU : Propylthiouracil

RGP : Radial Growth Pattern

VGP : Vertical Growth Pattern

ZFIN : Zebrafish Information Network

ACKNOWLEDGEMENTS

The studies presented here has been carried out at Izmir Biomedicine and Genome Institute, at Dokuz Eylul University between the period September 2016 to November 2018. I would be grateful to present and speak of all the people who contributed a lot to this study.

First of all, I would like to express my appreciation and gratitude to my supervisor and my mentor Dr. Güneş Özhan for giving me opportunity to study in her laboratory, for her continuous support and guidance throughout this study. She had faith in me even the times that my motivation was broken. I specially thank to the supervisor of IBG Zebrafish Facility Dr. Gülçin Çakan Akdoğan for sharing her in-depth knowledge with me during my studies. She showed patience throughout the experiments. Besides, I owe thanks a lot to our lab technician Ebru Turhanlar for her technical support.

I also would like to thank to Dr. Adam Hurlstone for sharing *mitfa*-/- (*nacre*); *kita*-GFP-RAS^{G12V} zebrafish line that really contributed much to the progression of the studies. I also want to thank Gözde Alkan for her helps in histology process. Additional thanks to my lab friends Yeliz Garanlı, Özgün Özalp, Yağmur Azbazdar, Gökhan Cucun, Özge Çark, Betül Haykır and İsmail Küçükaylak for always being supportive and helpful. I don't know how two years would pass without friendships of Ece Sönmezler, Yağmur Toktay, Elmas Nur Yılmaz and Mehmet Ergüven. I am very lucky to have them in my life. Last but not least, I want to thank to my parents who always supported me in my whole life. I would like to also speak of my little hairball Kavun for giving his endless love and fluffy paws to me.

COMPARISON OF THE MOLECULAR MECHANISMS OF MELANOCYTE REGENERATION AND MELANOMA USING THE ZEBRAFISH

Esra Katkat, Dokuz Eylul University Izmir International Biomedicine and Genome Institute, esra.katkat@ibg.edu.tr

ABSTRACT

Molecular mechanisms underlying regeneration and cancer have always been a challenging question. Studies that seek an answer to the common/different behaviors of these distinct processes are rare. Early regeneration involves rapid but controlled proliferation of progenitor cells. However, the clear distinction between regeneration and cancerization appears to happen as regenerating cell population decelerate proliferation, lose migratory features, mesenchymal characteristic and acquire differentiation, in a way unlike cancer cell population. Therefore, we hypothesized that molecular mechanism shared by cancerization and regeneration is similar at early stages whereas the cellular mechanisms must become dissimilar at the later stages. We used adult zebrafish as a model to test our hypothesis because it has high pigment regeneration capacity and rapid melanoma growth upon transgenic approaches. Besides, many tumor suppressors and oncogenes are conserved between zebrafish and human. We established melanocyte regeneration and melanoma models of zebrafish on caudal fin. We ablated melanocytes in adult zebrafish by Neocuproine (NCP) and determined early and late stages of melanocyte regeneration as one dpa and seven dpa, respectively. We used mitfa-/- (nacre); kita:GFP-RAS^{G12V} line to generate melanoma models. Within two months, both hyper-pigmented and hypo-pigmented melanoma arose in crossbreeds of mitfa-/- (nacre); kita:GFP-RAS^{G12V} and wild type (AB). We checked the expression levels of early and late melanocyte regeneration markers and neural crest cell markers for zebrafish melanoma. We found out that differentiation markers were high in hyper-pigmented melanoma while neural crest cell markers were high in hypo-pigmented melanoma. All in all, these observations may provide ground for the studies that would investigate melanocyte regeneration and melanoma on zebrafish model.

Keywords: Melanocyte, Melanoma, Regeneration, Zebrafish, Early and Later Stages

ZEBRA BALIĞININ MODEL ORGANİZMA OLARAK KULLANILARAK MELANOSİT REJENERASYONU VE MELANOMUN MOLEKÜLER MEKANİZMALARININ KARŞILAŞTIRILMASI

Esra Katkat, Dokuz Eylül Üniversitesi İzmir Uluslararası Biyotıp ve Genom Enstitüsü, esra.katkat@ibg.edu.tr

ÖZET

Rejenerasyon ve kanserin benzer veya farklı davranışlarına dayanan çalışmalar nadir olmasına rağmen, bu iki sürecin altında yatan moleküler mekanizmalar her zaman için ilgi konusu olmuştur. Kanser hücrelerinin aksine rejenerasyonun geç aşamasında yenilenmekte olan hücreler çoğalma, göç, mezenkimal özelliklerini kaybederken farklılaşma fenotipi artmaya başlar. Bu nedenle, kanser ve rejenerasyon tarafından paylaşılan moleküler mekanizmanın erken aşamalarda benzer olduğu, geç aşamalarında ise farklı olduğu hipotezini kurduk. Hipotezimizi test etmek için yetişkin zebra balığını model organizma olarak kullandık. Yüksek rejenerasyon potansiyeli ve transgenik yaklaşımlarla hızlı tümör indükleme avantajlarından dolayı zebra balığı, hipotezimizi test etmek için pratik bir model organizma olma özelliği göstermektedir. Bunun yanında, birçok onkogen ve tümör baskılayıcı genler insan ve zebra balığında korunmuş haldedir. Rejenerasyon modeli için Neocuproine (NCP) ile melanositleri öldürdük, melanosit rejenerasyonunun erken ve geç evrelerini belirledik. mitfa-/- (nacre); kita:GFP-RAS^{G12V} zebra balığı hattını, melanom modellerini oluşturmak için kullandık. İki ayda melanom geliştiğini gözlemledik. Farklılaşma genlerinin pigmentli tümörlerde yüksek, nöral krest genlerinin ise pigmentsizlerde yüksek olduğunu gördük. Pigmentli ve pigmentsiz tümörlerin geç aşama melanosit rejenerasyon genlerinde gösterdiği farklılıktan yola çıkarak pigmentsiz melanomun farklılaşma fenotipini kaybedip nöral krest/melanosit kök hücre genotipine ve fenotipine yaklaştığı sonucuna vardık. Sonuç olarak, bu iki süreci zebra balığında inceleyecek melanosit rejenerasyonu ve melanoma çalışmaları için zemin olabilecek sonuçlar ortaya koyduk.

Anahtar Kelimeler: Melanosit, Melanom, Rejenerasyon, Zebrabalığı, Erken ve Geç Evreler

INTRODUCTION

It has been demonstrated that the cellular pathways required for stem cell specification, lineage restriction and epithelial mesenchymal transition during embryo development and tissue regeneration are also common in tumorigenesis, although these processes are mediated in uncontrolled manner in cancer (Mani et al., 2008; Tse & Kalluri, 2007). Besides, the processes like self-renewal and cell proliferation, migration is also associated with several regeneration types which reminds the features of cancer. Even though the studies are rare in this topic, nowadays there is growing evidence that associate regeneration mechanisms with cancer biology.

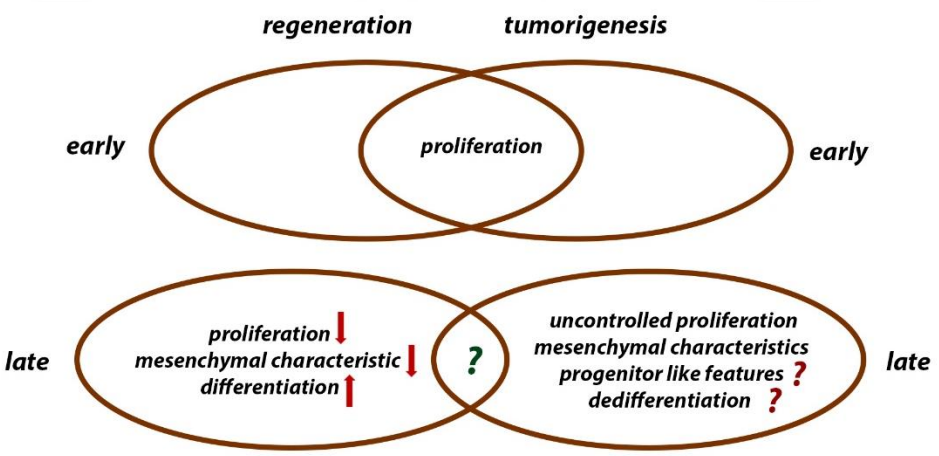

Figure 1.1 Diagram for early and late stages of regeneration and tumorigenesis. Molecular mechanisms of regeneration and tumorigenesis are similar at early stages while becoming dissimilar at their late stages.

Early regeneration involves rapid but controlled proliferation of progenitor cells. At later stages, regenerating cells decelerate proliferation, lose migratory features, lose mesenchymal characteristic and acquire differentiation. Similarly, tumorigenesis starts with proliferation of the cancer cells however in uncontrolled manner. Contrary to regeneration, progressed cancer maintains proliferation and mesenchymal phenotype at later stages (Fig1.1). Some phenotypic and molecular observations brought forward the idea that tumor progression might lead less differentiated and more progenitor like state. Moreover, regeneration and tumorigenesis could be molecularly related to each other, yet mostly overlooked because they are accepted as extremely distinct processes. If so, cancer can be thought as a wound that do not heal. At least, up to a certain stage it must show parallelism with regeneration and must show divergence after a certain stage at mechanistic level. These observations rationalize a potential link between

regeneration and cancer. The molecular similarities at early stages and divergence at later stages of both cellular contexts constitute the hypothesis of this study. The aim and the significance of this study is to investigate the molecular mechanisms at the transcriptional level by comparing single cell type (melanocyte) regeneration and melanoma at early and late stages.

1.1. Regeneration

Regeneration is the process by which some organisms in postembryonic life recover or restore the lost or amputated tissues, organs and functions. Regeneration could be either complete where the new tissue is the same as the lost tissue (eg. axolot limb) or incomplete where the necrotic tissue becomes fibrotic (eg. Wound healing). The origins of cells that participate in regeneration has been always a question. Answers to this question are different depending on the species, organs and tissues. Previously, regeneration was categorized based on proliferation. Two major classifications have been suggested by Morgan; regeneration that takes place without active cell proliferation (morphallaxis) and regeneration that requires cell proliferation (epimorphosis) (Morgan, 1898). In fact, regeneration is much more than cell proliferation; cell origins that participate regeneration should be also considered to categorize regeneration. Recently, four possible cell origins have been proposed in animal regeneration; a) activation of resident stem cells, b) direct proliferation of differentiated cells, c) dedifferentiation of mature cells or d) transdifferentiation of differentiated cells into another type (Fig.1.2).

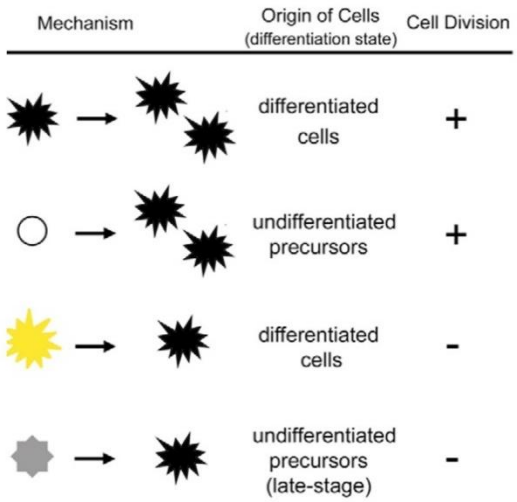

Figure 1.2 Four possible cell origins that participate in regeneration (Yang & Johnson, 2006).

Regeneration take place in four major ways in which various cells of origin participate:

Stem-cell mediated regeneration: Stem-cell mediated regeneration takes place through self-renewal of resident stem cell which are not terminally differentiated. Stem cells have two fates due to asymmetric division each daughter. They either commit a differentiation fate or remain as stem cell (Alberts, B. et al., 2002, pp. 1219–1220). Stem cells are critical in regeneration of various tissues. For example, hematopoietic stem cells in the bone marrow replace blood cells continuously and follicular stem cells are involved in hair shaft regeneration (Gilbert, 2014, p. 560). Resident stem cells or lineage restricted progenitors are also involved in stem cell mediated regeneration. In this type of regeneration lineage restricted precursors directly differentiate without proliferation to produce different type of cells (Carlson, 2007, p. 34). For example, zebrafish fin regeneration is built on nine different cell lineages in which all cell types are derived from distinct restricted progenitors (Tanaka & Reddien, 2011).

Compensatory regeneration: Compensatory regeneration can be defined as the proliferation of the pre-existing differentiated cells in the event of damage or loss, resulting in a complete functional organ (eg. human liver regeneration) (Carlson, 2007, p. 26).

Trans-differentiation of differentiated cells into another cell type (morphallaxis): Morphallaxis regeneration is driven directly from reorganization/trans-differentiation of the pre-existing cells without active cell proliferation. For example, hydra regeneration involves the direct reorganization/trans-differentiation of the pre-existing cells (Holstein & David, 1991; Park, Ortmeyer, & Blankenbaker, 1970). The existing cells in hydra regeneration, mostly under starvation conditions, is accomplished by tissue morphogenesis in which differentiated cells moves to proper sites and trans-differentiate to another cell types to complete regeneration (Siebert, Anton-Erxleben, & Bosch, 2008; Tanaka & Reddien, 2011).

Dedifferentiation of mature cells (epimorphosis): Epimorphosis is mediated by blastema formation and active cell proliferation. After injury or lost, new structures are formed through epimorphosis by dedifferentiation phase is required to form undifferentiated cell which will then proliferate and differentiate into new cells (Neurosurg, Zool, & Neurol, 2007). Epimorphosis is further subdivided into two distinct categories as blastema based epimorphosis and non-blastema based epimorphosis. Blastema based epimorphosis involves formation of blastema structure which is similar to early embryonic limb buds and is common to planarians, mollusks, gastropods and vertebrates (Sánchez Alvarado, 2000). On the other, mostly internal structures like bones and muscle undergoes non-blastema mediated epimorphosis.

1.2. Links Between Regeneration and Cancer

The argument about mechanistic link between cancer and regeneration has been first brought forward by Waddington. He proposed that the cells in individuation field, where developmental and regenerative activities are high, are less prone to cancerization. However, once the normal growing tissue escaped from the growth controlling agents, it becomes more prone to cancerization (Waddington, 1935). The studies of regeneration and cancer mostly conducted on newt, salamander and axolotl showed that the body regions (eg. limbs and tails) with high epimorphic regeneration capacity show resistance to tumor induction when compared to body sites with low regeneration capacity (Tsonis & Eguchi, 1982). Under normal conditions, regeneration follows a common route of injury-induced events that include cell proliferation, migration, differentiation and morphogenesis to restore tissue integrity and function. Most importantly, these events are terminated in a controlled manner so that the regenerating tissue does not transform into a mass of cells that undergo uncontrollable proliferation.

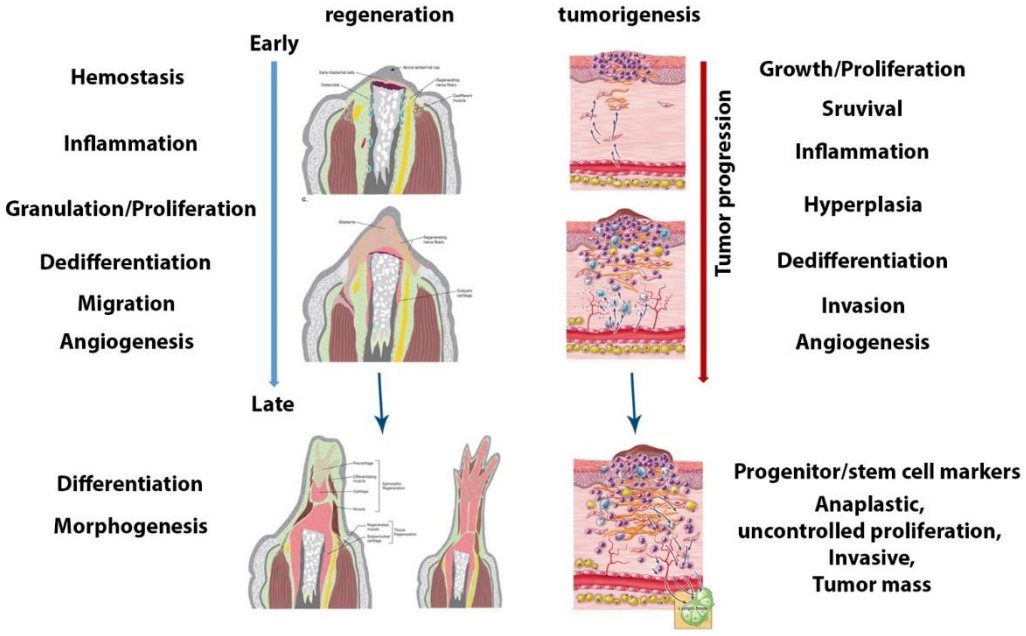

Figure 1.3 Phenotypic links between regeneration and tumorigenesis (Carlson, 2007; Norton, 2018).

Through regeneration (Fig.1.3), firstly hemostasis occurs by re-epithelization. In this phase keratinocytes and fibroblasts migrate and proliferate at the wound edge, leading to epithelization. Then blastema forms at the distal end of the stump, giving granulated appearance. Blastema can be defined as a mass of proliferating undifferentiating cells. Blastema formation is established by dedifferentiation of pre-existing differentiated cells. Then these

differentiated cells move distal end and redifferentiate to reconstitute morphogenesis (Carlson, 2007).

The cellular similarities between granulated wound site and tumor led cancer to be described as wounds that do not heal (Riss et al., 2006). Number of studies supported the hypothesis that describe cancer as wounds that do not heal regarding inflammatory response, angiogenesis and differential expression of genes related to cell proliferation, survival and migration (Crusz & Balkwill, 2015; Dipietro, 2013; Karin & Clevers, 2016). Granulation appearance is formed at the wound site due to blood-vessel sprouting, new vasculature development and deposition of matrix produced by fibroblasts (Carlson, 2007, pp. 8–10). Neovascularization, the formation of new blood vessels from pre-existing vessels, is crucial for both tumor growth and wound healing. Both processes require supply of oxygen and nutrients to be proceeded. For decades, inhibition of angiogenesis has been used as an effective cancer treatment strategy (Ferrara & Kerbel, 2005; Paavonen, Puolakkainen, Jussila, Jahkola, & Alitalo, 2000).

Inflammation and angiogenesis are essential for both blastema and tumor formation. The first phase of new tissue formation needs inflammatory cells to produce some factors like cytokines, growth factors and proteinases which induce migration and hyperproliferation of the keratinocytes to the wound site so that new epidermis and new vasculature can be formed there (Schäfer & Werner, 2008). Rudolf Virchow, based on several clinical observations, reasoned that defects in wound repair, non-healing ulcers and chronic inflammations could be the preconditions for tumor formation. Gastric infection caused by Helicobacter pylori can be an example of increased risk of gastric adenocarcinoma (Dunham, 1972). Besides clinical observations, experimental studies based on the earliest studies done by Peyton Rous also support this hypothesis. Chickens infected by Rous sarcoma virus which develop chronic inflammation is followed by tumor formation at the site of infection (Dolberg, Hollingsworth, Hertle, & Bissell, 1985). High incidence of such cases suggests that transformation of a healing wound into a malignant tumor arise due to common molecular and cellular mechanisms that are active in both wound healing and tumorigenesis (Dvorak, 1986; Haddow, 1973).

It is important to know the hallmarks of the cancer to compare with regeneration. One of the hallmarks of cancer is sustained proliferation (Hanahan & Weinberg, 2000). There are many ways that cancer sustain proliferation; including producing their own growth factors, increasing the number of growth factor receptors, deregulated intracellular pathways (e.g. Ras oncogenic

activation), inactivated tumor suppressor genes (e.g. RB, p53) (Bhowmick, Neilson, & Moses, 2004; Hanahan & Weinberg, 2011; Mani et al., 2008). Regeneration is controlled by intracellular mechanisms and signals from micro-environment in such a way that cells know when to proliferate, migrate and terminate these events. While regeneration process involves distinct modes of cell origins, cell proliferation is the prominent event in most of the early regeneration process (Dvorak, 1986; Haddow, 1973). Proliferation of resident progenitor cells or differentiated progeny is essential to replenish a group of stem cells in the tissue and to supply the regenerating tissue (Carlson, 2007, pp. 42–43).

The most important feature of the cancer that is related to invasion and metastasis is epithelial to mesenchymal transition (EMT). EMT is also frequently seen in early embryonic development and in the migration of keratinocytes to the injury site. Cancer cells acquire an EMT morphology in which they lose all cell-cell contact and start to invade other tissues in uncontrolled manner (Mani et al., 2008; Tse & Kalluri, 2007). For example, β1 integrins is involved in migration and proliferation of both wound keratinocytes and carcinoma cells. However, keratinocytes involved in wound repair reverts back to epithelial phenotype from mesenchymal-like phenotype whereas invasive cancer cells do not shut down mesenchymal phenotype and keep less differentiated phenotype (Grose, 2002).

Interestingly, in some respect tumorigenesis resemble the blastema formation that takes place through epimorphic regeneration. Furthermore, it is noteworthy to highlight that both processes resemble each other in respect to involvement of undifferentiated and dedifferentiated group of cells (Visvader, 2011). In dedifferentiation phase of regeneration, mature cells lose their differentiated characters and become more like a stem cell to participate in regeneration process. For example, cardiomyocytes in zebrafish heart during the regeneration process are dedifferentiated. Another good example is that the cell adjacent to wound is dedifferentiated to complete limb regeneration of amphibian urodeles (Jopling, Boue, & Belmonte, 2011). Similarly, in tumor bulk, there are a few cells called cancer stem cells that have capacity to give rise to a heterogenous tumor population by self-renewing and differentiating (Visvader, 2011). Besides, it has been found that the expression of differentiation markers in tumors are diminished gradually at early stages whereas expression of stem/progenitor markers increase at the later stages (Friedmann-Morvinski et al., 2012).

1.3. Melanocytes as a Platform to Compare the Regeneration and Cancer

1.3.1. Melanocyte Biology

Melanocytes are melanin-producing specialized cells and are derived from multipotent neural-crest cells. Melanocytes are mostly located in basal layer of the skin and hair follicles of the animals; however, they can be also found in several parts of the body including RPE, cochlea, brain, heart, lung and adipose tissue (Cichorek, Wachulska, Stasiewicz, & Tymiska, 2013). Melanin is produced in a specialized organelle called melanosome because of the toxicity of byproducts that emerge by melanogenesis (Fitzpatrick, 1961; Sulaimon & Kitchell, 2003). Melanosomes dispersion is provided by the active transport along microtubules to the tip of the dendrites from perinuclear area, from where they are transferred to nearby keratinocytes. Melanin granules are gathered around nucleus of the basal keratinocytes to give protection against UV ray. The protein content of melanosome includes tyrosinase, tyrosinase-related protein-1, dopachrome tautomerase (tyrosinase-related protein 2) and melanosomal matrix proteins (PMEL17, MART-1). TYR, TRYP1 and DCT are the three important enzymes required for melanin synthesis (Cichorek et al., 2013; Plonka et al., 2009).

There are two distinct types of melanin pigments produced in the mammalian body. The black-brown one is called eumelanin and yellow-reddish pigment is pheomelanin. The synthesis process of melanin pigments both pheomelanin and eumelanin begins with oxidation of tyrosine by tyrosinase to DOPA-quinones. The synthesis pathway determined by the existence of cysteine; the production of pheomelanin is produced in the presence of cysteine(Fig.1.4), whereas eumelanin is produced in the absence of cysteine (Cichorek et al., 2013).

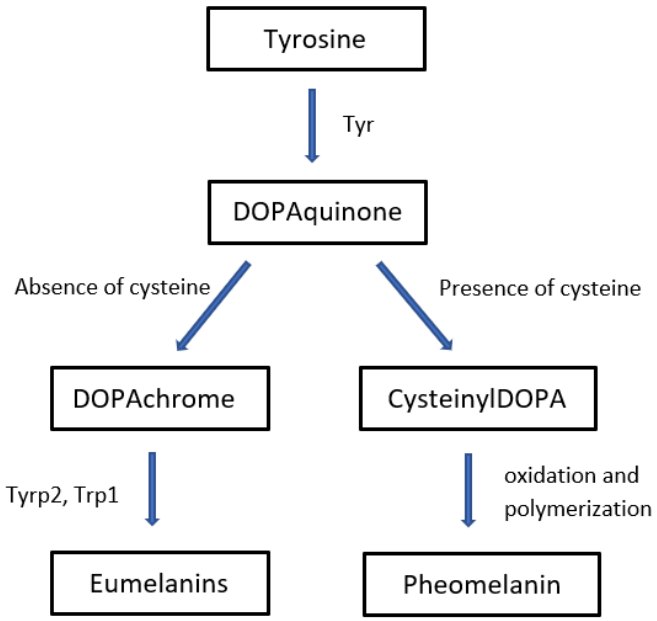

Figure 1.4 Schematic diagram of melanogenesis. In the first step tyrosine is transformed rapidly to DOPA quinone by tyrosinase. Lack of cysteine leads to production of eumelanin catalyzed by TYRP2 and TYRP1. On the other hand, pheomelanin is produced eumelanin through serial oxidation and polymerization processes in the presence of cysteine (Hearing, 2011; Sugumaran, 1991).

Mammalians have two groups of melanocyte population that are found in hair bulge and in skin between dermis and epidermis. Hair coloration is provided by transfer of melanin to growing hair. Growth (anagen), degeneration (catagen) and rest (telogen) phases constitutes hair follicle death and growth cycles (White & Zon, 2008). Melanocyte stem cells (MCSCs) are not alone in melanocyte regeneration, they co-occupy the hair follicle with epithelial hair follicle stem cells (HSCs) and act in synchrony during hair cycling (Rabbani et al., 2011).

Homogeneous pigmentation of mammalian skin is provided by distribution of melanin to nearby keratinocytes by melanocytes via their protruded dendrites (Fitzpatrick, 1961; Sulaimon & Kitchell, 2003). The continuous pigmentation of skin and hair is provided by *DCT*-positive stem cells. Melanocyte regeneration involves two main steps; self-renewal of stem cell and differentiation phase. WNT/beta catenin signaling plays an essential role in melanocyte regeneration at the beginning in which high levels of beta catenin increase *DCT* expression which leads to differentiation of the melanocyte stem cells. *WNT* alone is not the regulator of melanocyte regeneration. Additionally, *MITF*, *PAX3* and *SOX10* are involved in this process. *DCT* promoter contains enhancer sites that *MITF*, *SOX10* and *PAX3* bind and work in concert to mediate *DCT* expression. *PAX3* is associated with the repressed expression of *DCT* whereas *MITF* and *SOX10* promote *DCT* expression (Ceol, Houvras, White, & Zon, 2008).

1.3.2. Melanoma

Melanoma, an aggressive malignant tumor, is a type of skin cancer. There are also other types of skin cancer which includes basal cell carcinoma and squamous cell carcinoma. Even though melanoma account only 2.3 % of all skin cancer types, it constitutes 75% of all skin cancer related deaths (Bergman & Gruis, 2010; Garbe et al., 2016). Melanoma arises from the cells of melanocytic lineage and can be developed in various tissues. Mucosal surfaces and eye also carry the risk of melanoma development even though melanoma frequently is observed in the skin. Melanomas are mostly pigmented tumors, however amelanotic melanomas are also observed (Garbe et al., 2016).

Ninety percent of the death caused by melanoma is associated with cutaneous tumors that arise in the skin (Garbe et al., 2016). White populations face the highest incidence of melanoma development worldwide nearly 80%, in which Australia and New Zeeland have the highest incidence rate as 20-30 per 100.000 local people (Whiteman, Green, & Olsen, 2016). Melanoma had previously poor prognosis in the middle of 1900s. However, survival of patient that diagnosed with melanoma improved due to the increased awareness and early detection (Holly, Kelly, Shpall, & Chiu, 1987).

Melanoma subtypes are classified according to histopathological and clinical characterizations. Cutaneous melanoma has four types; superficial spreading melanoma, nodular melanoma, lentigo maligna and acral lentiginous melanoma. Other types of melanoma mucosal melanoma and ocular melanoma which have lower incidence rate. Ocular melanoma arises in the eye, and mucosal melanoma mostly occurs in the regions that has mucosal characteristics like body cavities, rectum, vagina (Prabhat Das, et.al., 2016).

Certain risk factors are defined to be involved in melanoma development. The risk of melanoma development is high in the individuals that have high numbers of dysplastic moles (nevi), nearly 25% of all melanoma cases is associated with preexisting nevi. Size and type of nevi significantly affect the risk of melanoma development, bigger size is related to increased risk (Bevona et al., 2003). Fair skin, personal or family history of melanoma, genetic susceptibility, UV radiation and severe sunburns also increase the risk of melanoma. People with darker skin develop melanoma less frequently than people with fair skin. The theory lies behind this scene is that UV irradiation would penetrate more easily and damage DNA through fair skin. Patients with family history of melanoma such as inherited mutations in tumor

suppressors (eg. CDKN2A, P16, P14) and oncogenes are also under the risk of developing melanoma (Prabhat Das, et.al., 2016).

Melanomagenesis and melanoma progression is a stepwise process which are associated with cumulative accumulation of mutations and sequential genetic alterations. Investigation of genetic contributors to melanoma nowadays is an important tool to understand and characterize melanoma. However, melanoma progression has long been characterized according to pathological and clinical studies as five stages which represents also metastatic transition: benign nevi; benign melanocytic nevi, atypical nevi (dysplastic nevi), primary malignant (RGP) melanoma, primary malignant (VGP) melanoma, and metastatic malignant melanoma (Fig. 1.5).

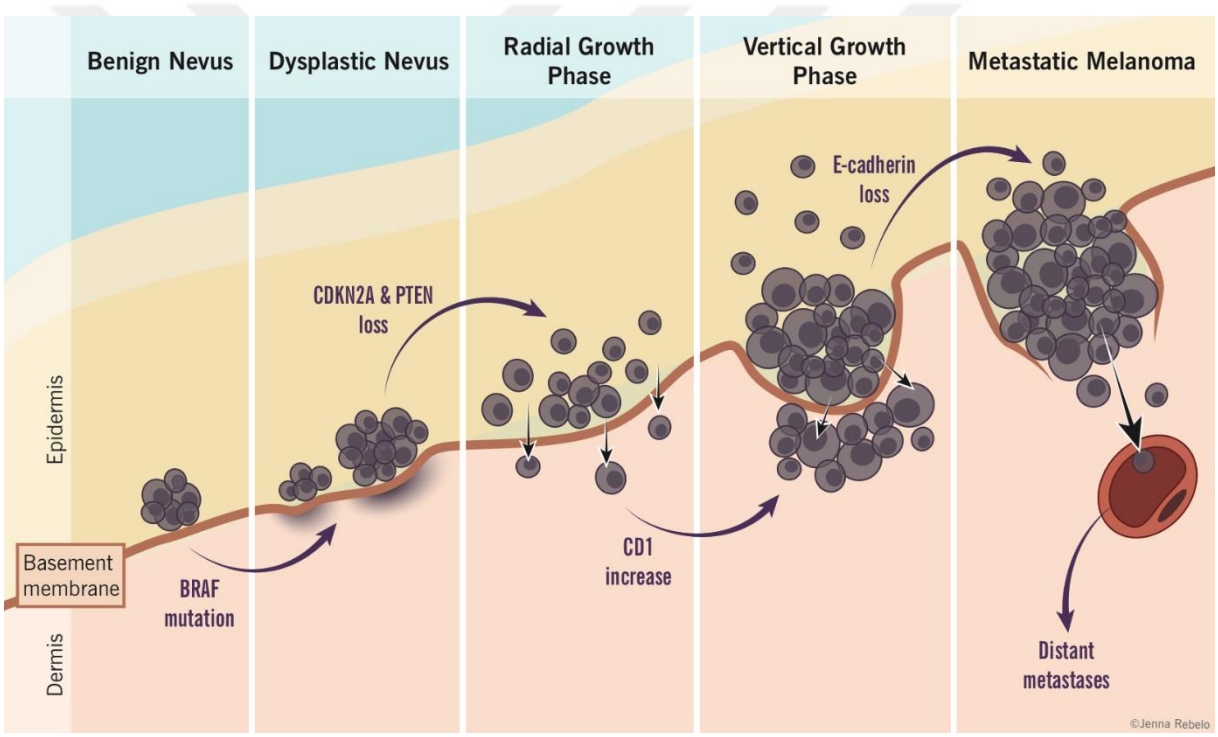

Figure 1.5 Schematic diagram of melanoma generation. Benign nevus has regular shape, resides mostly on the basement membrane between the epidermis and dermis. On the other hand, dysplastic nevus which are also called as atypical mole displays asymmetric morphology and irregular borders, yet dysplastic nevus are benign lesions. Once the cells acquired radial-growth phase characteristics it is melanoma. In this stage, melanoma cells grow horizontally through the basement membrane where they are mostly residing in epidermis layer. Vertical-growth phase is dangerous and decrease the survival rate dramatically since cells invade the dermis and find chance to get into lymphatic or vascular system (Seuradge & Wong, 2019).

As indicated previously, origin of melanoma could be either de novo transformation of melanocytes or could be congenital or inherited nevi. Pathology of melanomagenesis is complex due to involvement of many molecular events such as mutations, amplification, deletion, translocation and methylation of DNA. 8-12% of all melanomas is associated germline

mutation or deletion of tumor suppressor gene of cyclin dependent kinase inhibitor 2A gene (*CDKN2A*) leading aberrant regulation of cell cycle (Gruber, Ka, Brajac, Safti, & Peharda, 2008).

CDKN2A is responsible for coding two tumor suppressor proteins through alternative splicing; INK4A (P16) and ARF (P14). P16 inhibits CDK4/CDK6 complex that normally phosphorylate retinoblastoma protein (pRB). Retinoblastoma protein regulates cell cycle entry by binding and inhibiting E2F transcription factors. pRB function is directly or indirectly intersects with pathways controlling cellular senescence, apoptosis and DNA repair. Any alteration or mutations that leads to the production of nonfunctional pRB is associated with melanoma (Fountain et al., 1992; Schmidt, Ichimura, Messerle, Goike, & Collins, 1997; Serrano, Hannon, & Beach, 1993). *CDKN2A* also encodes ARF (P14) protein that plays an essential role in p53 regulation. ARF sequester MDM2 protein. If MDM2 is not sequestered by ARF, it would continuously direct P53 to proteasome for degradation, thereby p53 mediated apoptosis is ceased (Gruber et al., 2008).

BRAF mutation, which mostly leads to hyperactivation of BRAF and MAPK signaling pathway, is present nearly 50% percent of the melanomas. It is known that BRAF mutation is found in nevi and is related to hyper-proliferation of melanocytes. $BRAF^{V600E}$ is the most frequently seen mutation, accounting 90% of all BRAF mutations. In $BRAF^{V600E}$ mutation, as a result of T-A transversion glutamic acid replaces valine at the codon 600 which is located in kinase domain. This confers constitutive activation of RAF (Davies et al., 2002). *BRAF* mutation alone is not sufficient to generate melanoma, however together with additional mutations in tumor suppressor nevi progress to melanoma in nearly 4 months. Sporadic mutations of melanoma are frequently observed especially in protooncogenes that constitutively activates mitogen-activated protein kinase (MAPK) signaling pathway. MAPK signaling pathway is responsible for directing several cellular events such as cell survival, senescence, cell growth, cell migration and differentiation (Sebolt-Leopold & Herrera, 2004).

1.4. Zebrafish

1.4.1. Features of Zebrafish

Zebrafish (*Danio rerio*), a small teleost fish (bony fish), is classified in *Cyprinidae* family and mostly found in the Himalayan region of South Asia. The size of the Zebrafish is varied around 2.5-4 cm. Zebrafish, as an omnivorous, primarily feeds on insects and zooplanktons.

Their natural habitats are fresh waters including shallow ponds and lowland streams/rivers. The average life time of zebrafish that is living under controlled conditions has been reported as 42 months (Arunachalam, Raja, Vijayakumar, Malaiammal, & Mayden, 2013; Spence, Gerlach, Lawrence, & Smith, 2008). Although Francis Hamilton first described zebrafish in 19th century, the extensive use of zebrafish as a model organism came after 1960s. However, the early studies on zebrafish are done by Jane Marion Oppenheimer to understand vertebrate embryology and its developmental basics. She isolated halves of blastula from the *Danio rerio* egg and grafted to blastocoel of *Triturus torosus* eggs; she revealed that vertebrate body plan is promoted by a structure called organizer (Oppenheimer, 1936).

1.4.2. Advantages of Zebrafish

There are numerous reasons why zebrafish is convenient and powerful vertebrate model in the fields of biology including developmental biology, regeneration, cancer and neuroscience. Zebrafish can be used to model human diseases, screen pharmaceutics, perform toxicological studies and behavioral studies (Chakraborty et al. 2009). Husbandry and maintenance of the zebrafish is easy and cost-effective due to their tolerance to varying environmental conditions and their small sizes (Carpio Y. & Estrada, 2002).

Moreover, one female can lay large numbers of eggs at a time and within six days they can be ready for another mating. The average number of eggs they produce are around 150-200. Thus, this enables researchers to repeat the experiments several times for further verification. Even though in nature breeding season of zebrafish coincide with monsoon season which is from April to August (Spence et al., 2008), in laboratory conditions zebrafish can breed all year. Zebrafish embryo is relatively large and embryo development is rapid which enables to conduct and complete organogenesis experiments within five days post fertilization (dpf) Stages of embryogenesis and organ development can be visualized thoroughly due to transparency of embryo during the first 24 hours of development. Choice of tissues or cell types can be labeled with fluorescence proteins and their fates can be tracked throughout the development due to transparency. Besides, zebrafish has external fertilization and external development which led genetic manipulations to be done readily to produce transgenic and knock-out lines. Generation time is rapid; three months of zebrafish is ready for reproducing (Nüsslein-Volhard and Dahm, 2002).

Zebrafish genome was fully sequenced by the zebrafish genome project which was initiated by Sanger Institute in 2001 and completed in 2013. Zebrafish genome project revealed

that 70% of the zebrafish genome is similar to human. Through years of work and accumulated results, an online resource called ZFIN (The Zebrafish Information Network) has been established. ZFIN is a large database that provides information about zebrafish including anatomy, gene maps, sequence alignments, mutants and gene markers (Arunachalam et al., 2013). Several methods have been developed to increase efficiency and simplicity of transgenesis in zebrafish (*Gal4/UAS* system, *Tol2* system, heat shock system) (Kawakami, 2007; Shoji & Sato-Maeda, 2008; Urasaki, Asakawa, & Kawakami, 2008).

1.4.3. Zebrafish Regeneration

Regeneration capacity of mammals is poor when compared to lower vertebrates. During the evolutionary process some animals increased their regeneration capacity so that they can regenerate nearly all their organs and tissues (Dinsmore, 1991). These animal groups involve newts, hydra, salamanders, flatworms, urodele amphibians and teleost. On the other hand, mammals have poor regeneration capacity limited to some body parts like skin, blood, liver, muscle and bone. These body parts have the highest regenerative capacity also in humans yet is very poor when compared to lower vertebrates. Injury or loss in any organ and neurodegenerative diseases mostly lead to irreversible consequences in humans (Goessling & North, 2014; Poss, 2010; Tal, Franzosa, & Tanguay, 2010). Therefore, regeneration studies are attracting much attention and the molecular factors underlying the high regeneration capacity of these animals are being investigated. Although there are numerous model organisms used for regeneration studies, zebrafish due to its dynamic regeneration capacity is becoming increasingly popular on this field (Goessling & North, 2014). Zebrafish has ability to regenerate many organs and tissues including heart, pancreas, liver, muscle, skin, blood and pigment cells, fins and the central nervous system (CNS) (Goessling & North, 2014; Lush & Piotrowski, 2014; McCampbell & Wingert, 2014).

1.4.4. Development and Regeneration of Zebrafish Melanocytes

Melanocyte studies conducted on zebrafish dissected important molecular mechanisms required for melanocyte development and regeneration. Besides, these studies provided insights into the human melanocyte disorders (Plonka et al., 2009). Melanocytes are derived from neural crest cells which are induced at the border between neural and non-neural ectoderm during gastrulation. NCCs are a group of multipotent and migratory cells that give rise to distinct cell types (Erickson & Reedy, 1998). Gastrulation of neural plate is induced by the notochord that

lay beneath the neural plate. As the neural tube folds and closes, a group of cells undergo epithelial mesenchymal transition and delaminates from the edge of neural plate from the border between neural and non-neural ectoderm. The early specification of NCCs is provided by the activation of *bmp* and *notch* signaling. One of the important events that takes place through EMT is that the members of snail/slug family repress E-cadherin expression. Downregulation of E-cadherin leads detachment of NCCs from the epidermis (White & Zon, 2008). Next, NCCs migrate to different sites of the body to give rise distinct cell types such as Schwann cells, pigment cells, sensory and sympathetic neurons. NCC populations are grouped as cranial, vagal, sacral, trunk and cardiac depending on the sites they move. According to locations they move neural crests cells get gradual lineage restriction. The environmental factors that NCCs meet on migratory pathway also enhance their fates (Betters, Liu, Kjaeldgaard, Sundström, & García-Castro, 2010; Ernfors, 2010).

The melanocyte development starts with the specification of trunk and cranial neural crest cells to melanoblast lineages. Once melanoblasts are specified, they migrate to the proper sites and proliferate to give rise to mature melanocyte populations in the skin (Betters et al., 2010; Ernfors, 2010). There are two major pathways in the level of trunk neural crest migration; ventral pathway and dorsolateral pathway. The first migrating neural crest cells enter the ventral pathway while late migrating cells enters the dorsolateral pathway (Dupin & Le Douarin, 2003).

Melanocyte progenitors travel between the epidermis and the dermis, then enter ectoderm through the basal lamina. The expression of genes associated with melanocytic differentiation is increased as melanocytes travel to their final destinations. *mitf* is the master regulator of melanocyte differentiation and it regulates melanocytic differentiation markers through the differentiation process (Ernfors, 2010). *mitf* is involved in migration of melanocyte progenitors along dorsolateral pathway into the skin, in melanoblast specification and in pigment formation. Presence of *foxd3* inhibits *mitf* and leads to glial/neural precursor establishment. And after specification, melanoblasts upregulates ephrin and endothelin receptors so that they can migrate through extracellular matrix that has ephrin and endothelin (Fig.1.6). Precursors of glia/neurons are repelled by this pathway (Gilbert, 2014, pp. 379–380).

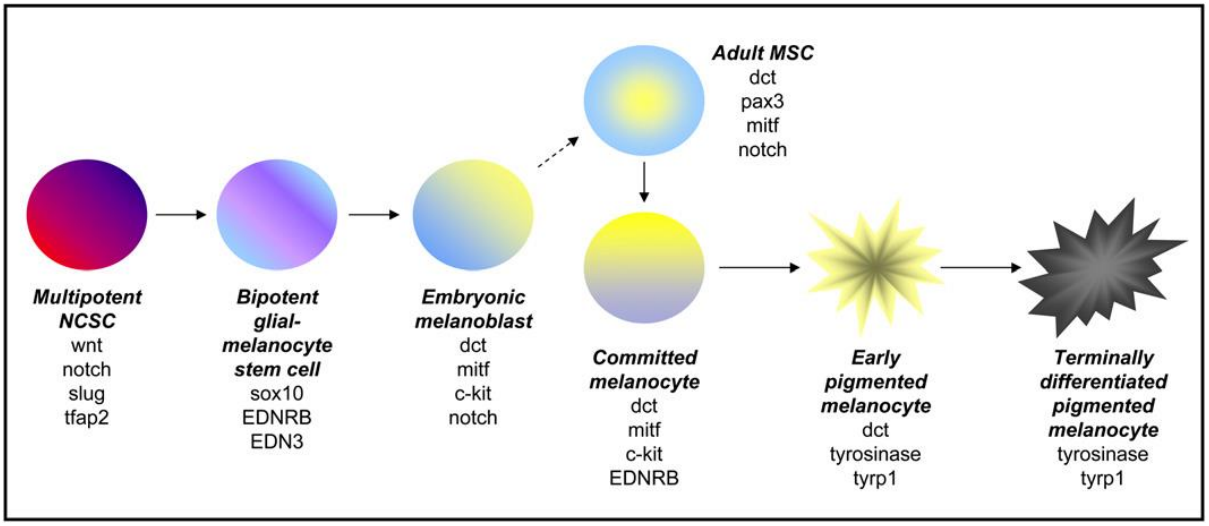

Figure 1.6 The stepwise melanocyte development from multipotent neural crest cells.

Melanogenesis starts before 24 hours post fertilization (hpf) and by 48 hpf the melanocyte pattern of zebrafish embryo is established (C. T. Yang, Sengelmann, & Johnson, 2004). Melanocytes do not constitute the pigment pattern of zebrafish alone. Xanthaphores and iridophores are other two pigment cells that constitutes zebrafish skin. The stripe pattern of zebrafish is established at the metamorphosis around two to four weeks. At the onset of metamorphosis, five dpf larval xanthophores proliferate and at three wpf iridophores along the horizontal myoseptum begin to appear. Melanophores start to appear around four wpf and stripe pattern of the juvenile fish is established at seven wpf (Johnson et al., 1995b).

Melanocyte regeneration of zebrafish has been well studied so far with the help of several ablation techniques. Laser ablation, chemical ablation (4-HA, MOTP, NCP), fin resection and NTR induced melanocyte death are widely used techniques to trigger melanocyte regeneration in zebrafish (Iyengar, Kasheta, & Ceol, 2015; O'Reilly-Pol & Johnson, 2008; C. Yang, Johnson, Yang, & Johnson, 2006; C. T. Yang et al., 2004).

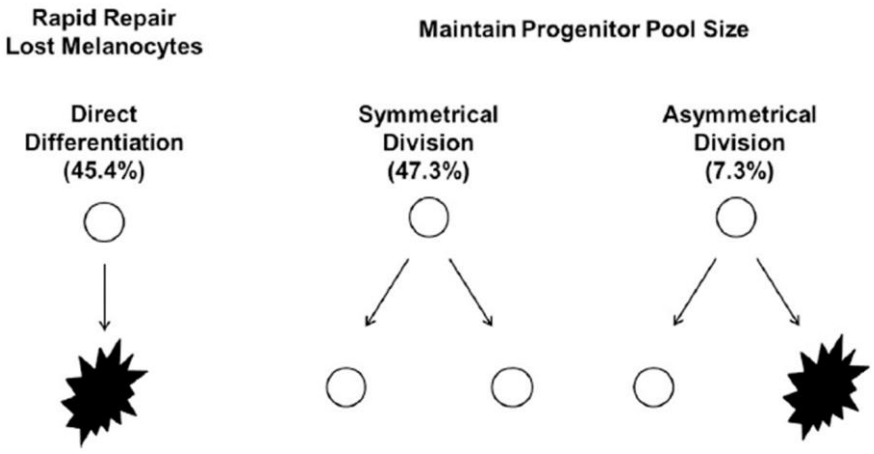

Figure 1.7 The three modes of melanocyte regeneration.

Melanocyte regeneration studies revealed that the supply of melanocyte progenitors is replenished inexhaustibly and melanocyte regeneration in zebrafish is mediated by the *mitf* positive unpigmented precursors that have homogenic distribution throughout the fin (Price, Weadick, Shim, Rodd, & Al, 2008; Rawls & Johnson, 2000). A subset of unpigmented *mitf* positive cells that undergo mitosis after ablation adopt distinct fates; direct differentiation, asymmetric division and symmetric division (Fig.1.7). Symmetric division replenish progenitor cells to keep MSCs reservoir. In asymmetric division, one daughter cell is differentiated and the other remained as *mitf* positive unpigmented precursor, in symmetric division both daughter cell maintain their unpigmented precursor states. The occurrence of asymmetric division is relatively lower than other types. Melanization starts between six to seven days after ablation and regeneration completes within four weeks (Iyengar et al., 2015).

1.4.5. Zebrafish Cancer Studies

Zebrafish is being increasingly a desirable model to study many of the cancer types. Cancer studies is easy and straight in zebrafish due to features mentioned above. Genetic homology and similar physiology to human, transparency of the embryo and larvae are some of the advantages of zebrafish in cancer studies. Histological, molecular and pathological characteristics of human and zebrafish cancer is similar in almost all tissue types. Moreover, oncogenes and tumor suppressor genes which are associated with signaling, DNA damage, apoptosis, and senescence pathways show high degree similarity between human and zebrafish (Amatruda & Patton, 2008). For example, oncogenes like *braf*, *nras* and *hras* are highly conserved in human and zebrafish that microinjections of human version of these oncogenes

under tissue specific promoters leads to highly penetrant tumors in zebrafish (Zhao, Huang, & Ye, 2015).

Zebrafish models are ideal to investigate angiogenesis due to similar vascular system to human and rapid growth of vasculature. Nearly at 24 hpf zebrafish vasculature is established. Transparency of larvae can be maintained for vascular system imaging till 14 dpf by PTU that prevents melanin synthesis by inhibiting tyrosinase. On the other hand, Casper mutant (roy_{a9}; $mitfa_{w2}$) that has deficiency in the development of iridophores and melanophores completely lack all melanocytes and iridophores. Thus, throughout embryogenesis and adulthood Casper line has transparent body such that even eggs in ovaries of female can be observed easily by naked eye. Also, most of the organs and internal body structures of Casper strain can be visualized under the microscope. Therefore, Casper line was developed as an excellent model to image even single cell level micro-metastases in vivo (Karlsson, von Hofsten, & Olsson, 2001). The other zebrafish strain which provides advantage in visualizing metastasis and in investigating angiogenesis is *Tg(fli:egfp)* zebrafish transgenic line. Vascular endothelial cells of *Tg(fli:egfp)* zebrafish line is labelled with GFP fluorescent protein under *fli* promoter (Chávez, Aedo, Fierro, Allende, & Egaña, 2016; White & Zon, 2008).

1.4.5.1. Mutagenesis and Transgenesis

Treatment of zebrafish with mutagens is easy because zebrafish can absorb dissolved chemicals directly from water. Exposure time, period and concentrations in water can be modified easily. Moreover, large numbers of fish can be exposed to a chemical at the same time. (Feitsma & Cuppen, 2008). Deletion or overexpression of the genes may lead to lethality of the fish and impede the stable line generation. Thus, tools that provides spatial and temporal control have been developed in order to overcome these drawbacks. Over-expression of oncogenes or knock-out of tumor suppressor genes are provided by methods such as *Gal4/UAS*, the Cre/lox, site specific recombinases, *Tol2* transposon and I-Sec to induce tumorigenesis (David M. Langenau, 2016, pp. 23–25).

The tol2 kit is designed to increase efficiency of zebrafish transgenesis. The system is based on tol2 transposition. The *Tol2* element first is discovered in the genome of Medaka fish and found to be autonomously active. DNA transposons are not naturally active in vertebrate genome despite the space they occupy, except for the medaka fish. The length of the *Tol2* element is about 4.7 kb and contains 4 exons that encodes transposase protein which is 649 aa in length. Transposase recognizes *Tol2* sites and catalyzes transposition of the *Tol2* construct

by cut and paste fashion. This method was adopted to zebrafish by introducing transposon-donor plasmid and transposase mRNA. These two constructs are injected fertilized zebrafish embryo. Transposase enzyme transcribed excises construct from the *Tol2* sites and integrates into the zebrafish genome randomly.

1.4.5.2. Xenotransplantation

Xenotransplantation models of zebrafish larvae are generated by transplantations of mammalian tumor cells to zebrafish larvae. Tumor cells are labeled with florescent dyes to visualize angiogenesis and track metastasis of different groups of tumor cells (Traver et al., 2003). Transplantation at early development of the zebrafish embryo, around 6-48 hours post fertilization, provides an advantage over other xenotransplantation models that zebrafish larvae do not develop the adaptive immune system till 14 days post fertilization. This feature of zebrafish larvae allows researchers to engraft human tumor cell without any immune suppression (Stoletov & Klemke, 2008). On the other hand, the dynamics of the microtumor formations and angiogenesis is much more efficiently investigated in 30-day-old zebrafish xenotransplantation model. This model is also advantageous due to completed development of major organs and vasculature when compared to developing embryo (Isogai, 2003).

1.4.6. Zebrafish Melanoma Studies

Zebrafish has been used as a robust animal to model many human genetic disorders related to pigmentation which includes Waardenburg Syndrome, albinism and piebaldism. Chemical or UV induced melanoma models have been established however transgenesis methods are more efficient and specific for melanoma generation in Zebrafish. *BRAF*, *KRAS*, *NRAS* and recently *HRAS* are the most widely mutated in human melanoma. Thus, several animal models for melanoma were established including Zebrafish melanoma model in order to investigate the role of those genes in melanoma initiation and progression (White et al., 2011). Regarding to histopathological examination, the melanoma promoted by *BRAF* and *p53* mutation in Zebrafish is similar to human melanoma (Amatruda et al., 2002). $BRAF^{V600E}/p53$ is the first zebrafish melanoma model generated by Patton and Zon in 2005 (Fig.1.8). This model is created by expressing $BRAF^{V600E}$ under the mitfa promoter. $BRAF^{V600E}$ over-expression is restricted to Zebrafish melanocytes and due to hyperproliferation of the melanocyte nevi like large ectopic melanocytic lesions are formed on adult Zebrafish (Patton and Zon, 2005).

Gene/ transgene	Line	Promoter	Cooperating mutation	Phenotype
$BRAF^{V600E}$	Stable and mosaic	*mitfa*		Nevi
$BRAF^{V600E}$	Stable and mosaic	*mitfa*	$tp53^{M214K}$	Melanoma
$HRAS^{G12V}$	Stable	*kita*		Hyperpigmentation, Melanoma
$HRAS^{G12V}$	Mosaic	*mitfa*		Nodule

Figure 1.8 Representative Zebrafish Melanoma Models (van Rooijen, Fazio & Zon, 2017).

The $BRAF^{V600E}$/miniCoopR system can be an alternative method to create Zebrafish melanoma model in which melanocytes are rescued in mosaic fashion. In this system, Patton et al developed a transgenic line *Tg(mitfa:*$BRAF^{V600E}$*;p53zdf1/zdf1)* and crossed to nacre mutant of zebrafish that carries inactivating mutation of *mitfa*. This triple transgenic lack all melanocytes and upon injection of miniCoopR vector which has mini-mitfa gene driven by mitfa promoter to embryos of this line, melanocytes are rescued in mosaic fashion. Rescued melanocytes carry *BRAF* and *p53* mutation which leads to melanoma development. This system allows additional genes to be expressed in rescued melanocytes in order to make functional screen for those additional genes (Patton, Mitchell, & Nairn, 2010)

An alternative method to induce melanoma in zebrafish is based on *RAS* oncogene. Nearly one third of the human primary and metastatic melanoma carry *RAS* mutations. Activating *NRAS* and *HRAS* mutations give rise to pigmentation abnormalities such as lost and dispersed stripe pattern, heavy pigmentation on fin and on scales. $HRAS^{G12V}$ mutation alone under *kita* promoter to induce hyperproliferation is sufficient to induce melanoma (Fig.1.8). On the other hand, melanoma generation with NRAS activating mutation is provided along with *INK4A* and *ARF/p53* mutation (Dovey, White, & Zon, 2009; Michailidou Et Al., 2009; Santoriello Et Al., 2010).

Zebrafish is now being practical model organism in wide range of laboratory studies. The studies conducted on pigment pattern of zebrafish provides an insight into the discovery of molecular mechanisms lay behind human pigmentation disorders. There exist several zebrafish mutants that display the dramatic effects of pigmentation disorders. For example, nacre carrying $mitf_{W2}$ mutation lack all melanocytes except retinal pigment epithelium (RPE) melanocytes. Not

all mutant zebrafish lack whole pigment type, some mutants have disrupted stripe pattern because of the mutation. For example, *ednrb* mutation in zebrafish leads to disrupted stripe pattern, in which melanocyte number is dramatically decreased and dark stripe is broken into melanocytic spots (Mahalwar, Singh, Fadeev, Nüsslein-Volhard, & Irion, 2016; Rawls, Mellgren, & Johnson, 2001). As a model organism zebrafish is an excellent organism to test our hypothesis. Studies of melanocyte biology are easy and robust in zebrafish in respect to easy visualization and quantification due to big size of melanocytes. Melanoma studies are well established on zebrafish with the help of rapid transgenesis tools and melanoma development is easily tracked due to its pigmented nature.

MATERIALS AND METHODS

2.1. Zebrafish Husbandry and Maintenance

Adult zebrafish are kept in special rooms in controlled conditions. An aquarium system, with 360 tank capacity, keep water temperature around 28°C, pH 7.4 and control salinity. The room lighting system is automatized for 12 light and 12 dark cycle in order to simulate day and night. Females and males are not kept in sperate tanks instead they are mixed in a way that five fish are present per L. System water are obtained from distilled UV treated water which is supplemented with several salts and sodium bicarbonate to imitate natural conditions. Embryos are kept in E3 medium till 6 days post fertilization (dpf) then transferred to system.

All research was conducted with the approval of IBG-HADYEK.

2.2. Breeding

Mating crosses are set up in the evening. Fish are transferred to breeding tanks that are 1 L in volume and equipped with removable sieves. Equal numbers of female and male fish are put into the separate parts of the tank. Tanks are left overnight and in the morning the barrier between females and males are removed. Within 30 minutes they mate, and females lay egg. A sieve at the bottom of the tank holds the eggs in a separate section from the fishes so that the fish do not eat the eggs. After spawn, eggs are collected into E3 containing 90 mm petri dishes with a strainer.

2.3. Embryo Bleaching

Embryos that are intended to be raised in the system are sterilized through bleaching at 1 dpf. Since 1 dpf chorion of the embryos are fragile, bleaching process is applied between 10 hpf-28 hpf. Five containers are set-up as in the following order; bleach bath, water bath, bleach bath, water bath and water bath. 230 µl NaOCl per 500 mL dH_2O is used to prepare bleach baths. Embryos which is in strainer are transferred to first bleach bath and incubated five minutes. Then, the embryos are incubated in each bath for 5 minutes. After the last wash, embryos are transferred to E3 medium in petri dish. Bleaching process is harsh and harden chorion. Thus, after bleaching process 10 µl pronase is added (30 mg/ml in E3) to each petri dish to for successful hatching.

2.4. Generation of Melanocyte Regeneration Models of Zebrafish

Neocuproine (NCP) which is a copper chelator was used for melanocyte regeneration studies in adult zebrafish. NCP specifically ablates adult zebrafish melanocytes by preventing tyrosinase activity and melanin synthesis (O'Reilly-Pol & Johnson, 2008). Zebrafish was subjected to one-day NCP treatment. NCP was washed after 24 hours. Caudal fin was resected at the days (1, 2, 3, 4, 7, 12, 15 and 20). The days between 1-4 dpa were investigated for early melanocyte regeneration. Subsequent days were investigated for late regeneration of melanocytes.

2.5. Drug Treatments

NCP (Sigma-Aldrich) was prepared as 25 mg/ml stock solutions by dissolving in DMSO. Final concentration of NCP was used as 1 μM. 1 mg/ml final concentration of Epinephrine (Sigma-Aldrich) was dissolved in 0.125 M HCl as 18mg/ml stock concentration (1 M). Fish were treated with epinephrine for 15-20 minutes prior to imaging at 1 mg/ml final concentration.

2.6. Generation of Zebrafish Melanoma Models

Two methods were followed to generate melanoma models of zebrafish. In the first *mitfa*-/- (*nacre*); *kita*:GFP-RAS^{G12V} zebrafish line received from Hurlston Lab. crossed with AB wild strain to obtain *Tg(mitfa+/-; kita-GFP-RAS^{G12V})* zebrafish breeds that shows overexpression *RAS^{G12V}* only in melanocytes. In the second, miniCoopR system was utilized to create the mosaic melanoma models by melanocyte rescue in *Tg(p53+/-; mitfa-/-; roy-/-; RAS^{G12V})* line.

2.6.1. Breeds of *mitfa*-/- (*nacre*); *kita*:GFP-RAS line and Wild type strain (AB)

The melanoma model that we employed is cross of wild type zebrafish line (AB) and *mitfa*-/- (*nacre*); *kita*:GFP-RAS^{G12V} to produce benign and malignant melanoma. Hurlston Lab. had generated first *mitfa*-/- (*nacre*); *kita*:GFP-RAS^{G12V} zebrafish line by raising *kita*:GFP-RAS^{G12V} zebrafish line in the background of *nacre (mitfa-/-)* strain. Melanocyte development in *nacre* zebrafish line is devoid due to *mitfa* loss of function mutation (J. Lister, Robertson, Lepage, Johnson, & Raible, 1999). When *mitfa*-/- (*nacre*); *kita*:GFP-RAS^{G12V} zebrafish line crossed with wild type (AB), the crossbreeds have heterozygous expression of mitfa which is enough for melanocyte development. The half of the breeds showed wild type phenotype due to one copy of *mitfa*. The other half showed hyperpigmentation all over the body due to hyperproliferation of melanocytes because of *RAS^{G12V}* overexpression (Figure 2.1.).

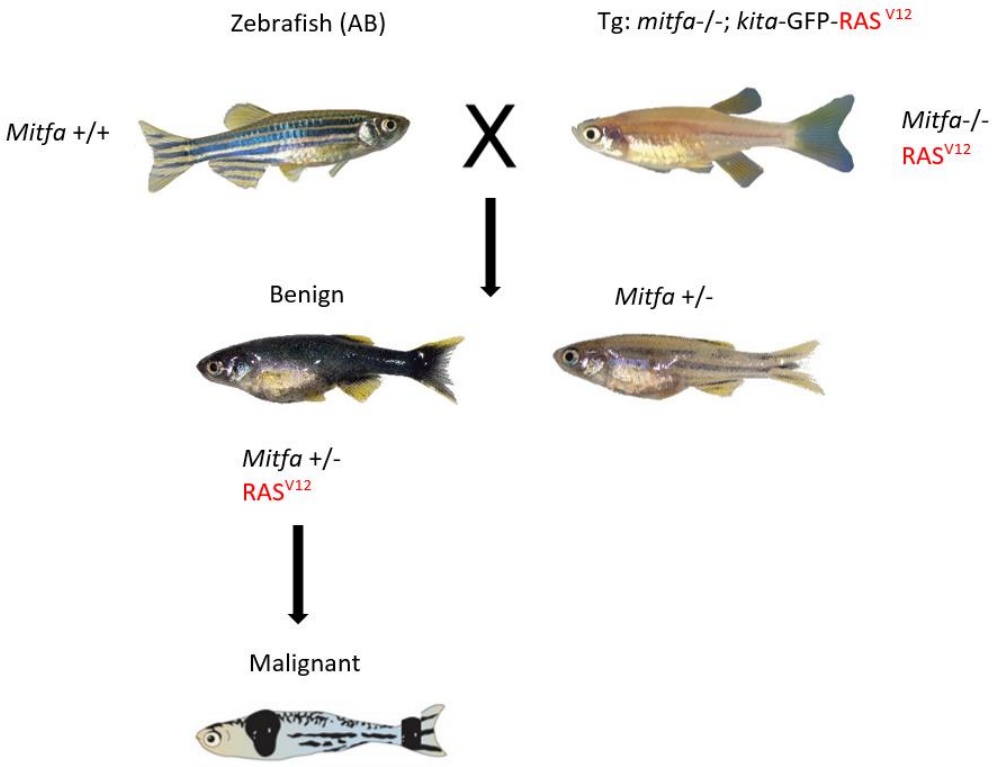

Figure 2.1 Zebrafish melanoma model by using *mitfa*-/- (*nacre*); *kita*:GFP-RAS^{G12V} line. Zebrafish melanoma model was produced by crossing Tg(*mitfa*-/-; *kita*:GFP-RAS^{G12V}) line to wild type (AB). The half of the progeny that acquire copy of mutated RAS^{G12V} show enhanced melanocyte pigmentation all over the body. The phenotype of other half seems like wild type zebrafish since they acquire one copy of *mitfa* and do not acquire RAS^{G12V}. Within 2-5 months later benign melanocytic lesions give rise to malignant growth of melanoma.

2.6.2. Melanoma generation in mosaic fashion; Gateway cloning strategy and *Tol2* transposition system

We used RAS^{G12V}/miniCoopR system as an alternative method to create Zebrafish melanoma model in which melanocytes are rescued in mosaic fashion. In this system, we exploited transgenic line *Tg(mitfa-/-;kita:GFP-RAS^{G12V})* line to obtain *RAS^{G12V}* overexpression in the *casper* background (*roy$_{a9}$; mitfa$_{w2}$*). Melanocytes are not developed in *casper* because of inactivating mutation of *mitfa* and *roy*. We crossed *Tg(mitfa-/-;kita:GFP-RAS^{G12V})* to *casper* to have *mitf-/-;roy+/-; RAS^{G12V}* progeny. Then, this progeny was back crossed to *casper* mutant to obtain *RAS^{G12V}* under *kita* promoter in the background of *casper* mutant. *mitf-/-;roy-/-; RAS^{G12V}* progeny does not develop melanocytes due to lack of *mitf* expression. However, injection of any construct that is carrying *mitf* gene to one stage cell embryo rescues melanocyte. Then, we crossed *mitf-/-;roy+/-; RAS^{G12V}* line to *mitf-/-;roy+/-; p53-/-* and injected MiniCoopR carrying plasmid to this progeny (Fig. 2.2). *RAS^{G12V}* overexpression leads to melanocytic overexpansion in larva beginning at 7 dpf.

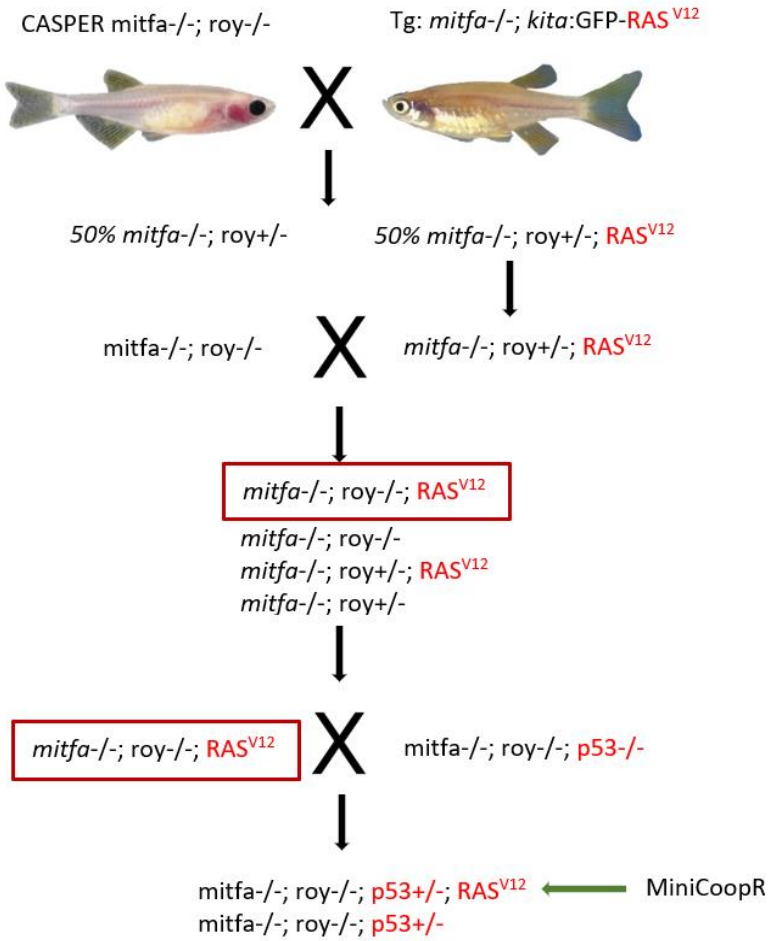

Figure 2.2 Generation of mosaic melanoma models of zebrafish. *mitf-/-;roy+/-; RAS^{G12V}* was produced by crossing *casper* to *Tg(mitfa-/-; kita:GFP-RAS^{G12V})*. Then, the progeny back-crossed to *casper* mutant to have *mitf-/-;roy-/-; RAS^{G12V}* fish. Injections were performed to progeny of *mitf-/-;roy-/-; RAS^{G12V}* in p53+/- background.

Cloning: We performed one stage cell embryo injections with the construct that is obtained through LR reaction. We used LR cloning to insert the required elements into a destination vector. This method led us to insert multiple DNA of interest into a destination vector. The name of the vectors and descriptions are in the following table (Table 2.1.). The constructs are either received from Ceol Lab and Hurlstone Lab or designed in our lab.

Table 2.1 The name of the vectors and descriptions.

Name	Description
pME-EGFP	Includes EGFP
p3E-polyA	Includes SV40 late poly A signal sequence from pCS2+
p5E-*mitf*	Includes *mitf* promoter
Destination vector-miniCoopR	Includes *mitf* gene

5’ entry clone (p5E-*mitf*) carries a promoter element called *mitf* which is active only melanocyte lineage and mature melanocytes. The *mitf* promoter is flanked by attL4/attR1 sites. 3’ entry clone (p3E-polyA) was designed to add a polyadenylation signal that are flanked by attR2/attL3 sites to the end of the gene. Middle entry clone (pME-EGFP) carry a fluorescence reporter gene (EGFP) flanked by attL1/attL2 sites. The destination vector (MiniCoopR, Hurlstone lab) was designed to have *mitf* gene. MiniCoopR vector carries three basic features; *Tol2* transposon ends, a multisite Gateway cloning cassette (attR4-ccdB-cmR-attR3) and polyA signal. The Gateway cloning cassette is important for negative selection with ccdb gene for non-recombined vectors. A ccdB cassette produces a bacterial toxin that poisons DNA gyrase and plasmids containing ccdB gene cannot be propagated in standard E. coli strains. If LR reaction is unsuccessful, ccdB cassette cannot be excised from the destination vector; as a result, bacteria that contain plasmid with ccdB cassette will be eliminated. On the other hand, if LR reaction is successful, bacteria that take the expression clone would survive on the amp LB.

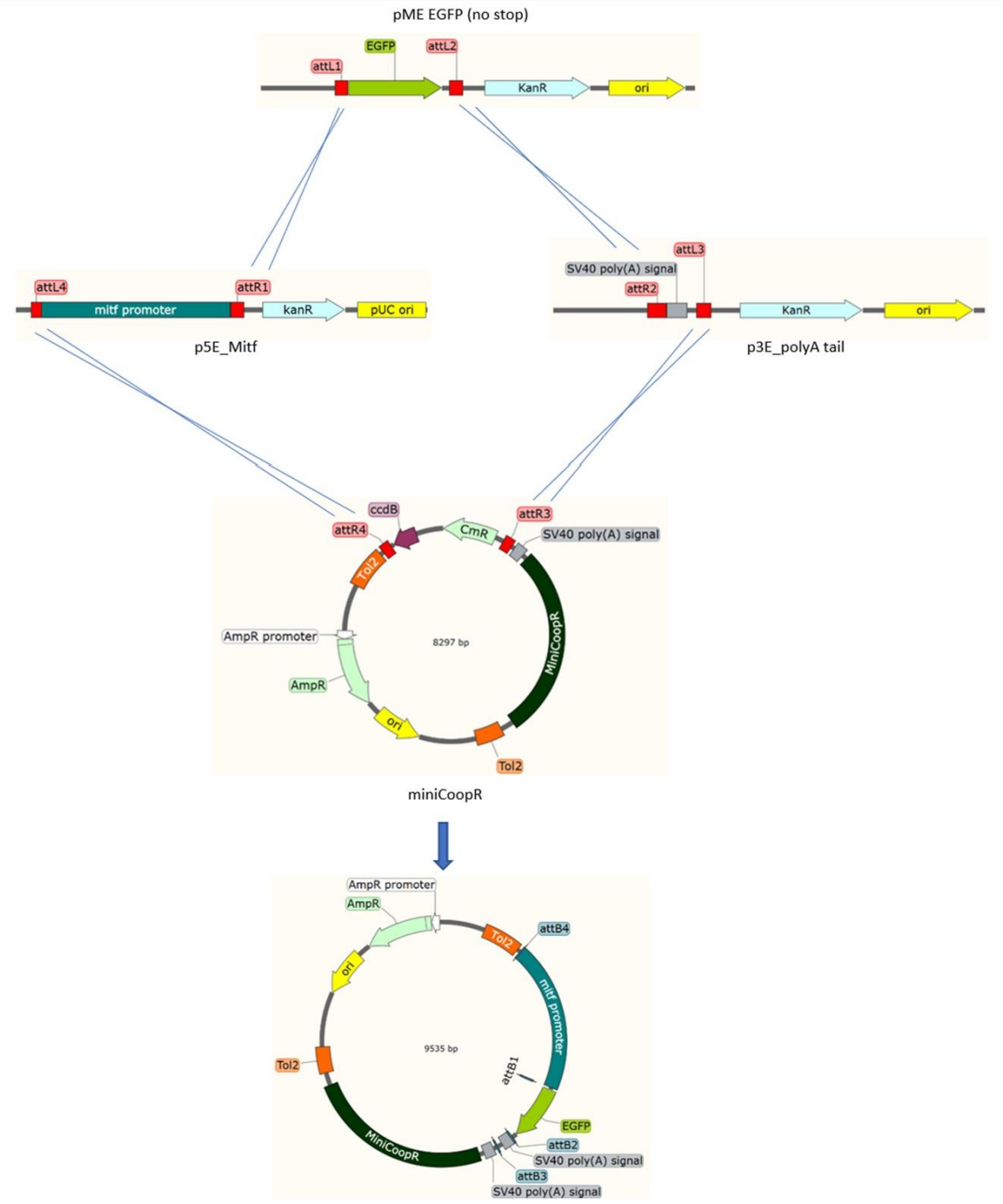

Figure 2.3 Gateway cloning strategy. The LR cloning was performed with the 3 entry clones and a destination vector to obtain expression construct. Entry clones are pME-EGFP, p3E-polyA and p5E-*mitf*. The LR reaction takes place between the specific att sites in which DNA segments flanked by the att sites are switched; attL1 site combines with attR1, attL2 site combines with attR2, attL3 site combines with attR3, attL4 site combines with attR4. attL sites are cut with the recombination protein (LR clonase) and ligated to the corresponding attR sites to create expression clone. In this LR reaction EGFP, mitf promoter, polyA were inserted to destination vector carrying MiniCoopR (mini *mitf* gene). The region between attR4 and attR3 (CmR, ccdb) on destination vector was discarded through LR reaction and EGFP, *mitf* promoter, polyA were inserted between these sites. The attL recombination sites then turned into attB recombination site after the reaction.

Materials required for LR reaction are entry clones (50-150 ng/µl in TE, pH 8.0), destination vector of choice (150 ng/µl in TE, pH 8.0), LR Clonase enzyme mix, TE Buffer, pH 8.0, pENTR™-gus positive control, 2 µg/µl Proteinase K solution, appropriate competent E. coli host, S.O.C. Medium, LB agar plates with the appropriate antibiotic to select for expression clones. LR recombination was set up with the following components (Table 2.2.) in 1.5 ml microcentrifuge tubes at room temperature and was incubated at bench overnight. The pENTR™-gus plasmid was used as positive control that will generate an expression clone which would be expressing β-glucuronidase (gus).

Table 2.2 LR recombination reaction set up.

Component	Sample	Negative Control	Positive Control
Entry clone (100-300 ng/reaction)	1-10 µl	--	--
Destination vector (300 ng/reaction)	2 µl	2 µl	2 µl
pENTR™-gus (50 ng/µl)	--	--	2 µl
5X LR Clonase™ Reaction Buffer	4 µl	4 µl	4 µl
TE Buffer	to 16 µl	10 µl	8 µl

Then the LR reaction product was proceeded with transformation. Chemical or electrocompetent TOP10 were used for transformations. Materials that were used for chemical and electrocompetent transformation as in the following table (Table 2.3.).

Table 2.3 Materials used for chemical and electrocompetent transformation.

Chemical competent	Electrocompetent
BP recombination reaction	BP recombination reaction
TOP10	TOP10
LB plates with the appropriate antibiotic	LB plates with the appropriate antibiotic
42°C water bath	Electroporator
37°C shaking incubator	37°C shaking incubator
Positive control	Positive control
S.O.C. medium	S.O.C. medium

Chemical transformation: 1 µl of the LR reaction was added into the tube containing 50 µl of competent cells. BP reaction and competent cell mix were incubated on ice for 30 minutes.

Cells were heat-shock at 42°C for 45-60 seconds then immediately transferred to ice. For recovery, 450 µl of room temperature S.O.C. medium was added and shaken at 200 rpm at 37°C for 1 hour. 2 Pre-warmed Amp LB plates were spread by 50 µl and 450 µl from each transformation and incubated overnight at 37°C.

Electrocompetent transformation: 1 µl of the LR reaction was added into a 50 µl of electrocompetent E. coli and mixed gently. Then, the mix is transferred to cuvette. By using electroporator the mix was electroporated and immediately 450 µl of room temperature S.O.C. medium was added into the mix. The mix then was transferred to 1.5 mL microcentrifuge tubes for recovery at 200 rpm at 37°C for 1 hour. 2 Pre-warmed Amp LB plates were spread by 50 µl and 450 µl from each transformation and incubated overnight at 37°C.

***Tol2* transposase capped mRNA synthesis in vitro transcription:** *Tol2* transposase capped mRNA was obtained by mMESSAGE mMACHINE® Kit. Large amounts of capped RNA can be produced through in vitro synthesis. Eukaryotic cells have a 7-methyl guanosine cap structure at 5', which protects termini of mRNA against several nucleolytic enzymes. In vitro synthesis kit is designed to add an analog cap [m7G (5') ppp (5') G] at 5'.

pCS2FA-transposase (KMK, Kristen Kwan, Chien lab) vector which is found in Tol2kit set was used to obtain capped transposase mRNA. Vector was first linearized by restriction enzyme. SP6 promoter followed by transposase gene was used as template for in vitro transcription. Vector linearization is required due to high processive characteristics of RNA polymerases which could generate long, heterogeneous transcripts that has low efficiency. Vector was linearized downstream of the polyA tail because in vitro synthesis would continue if 3' is not terminated.

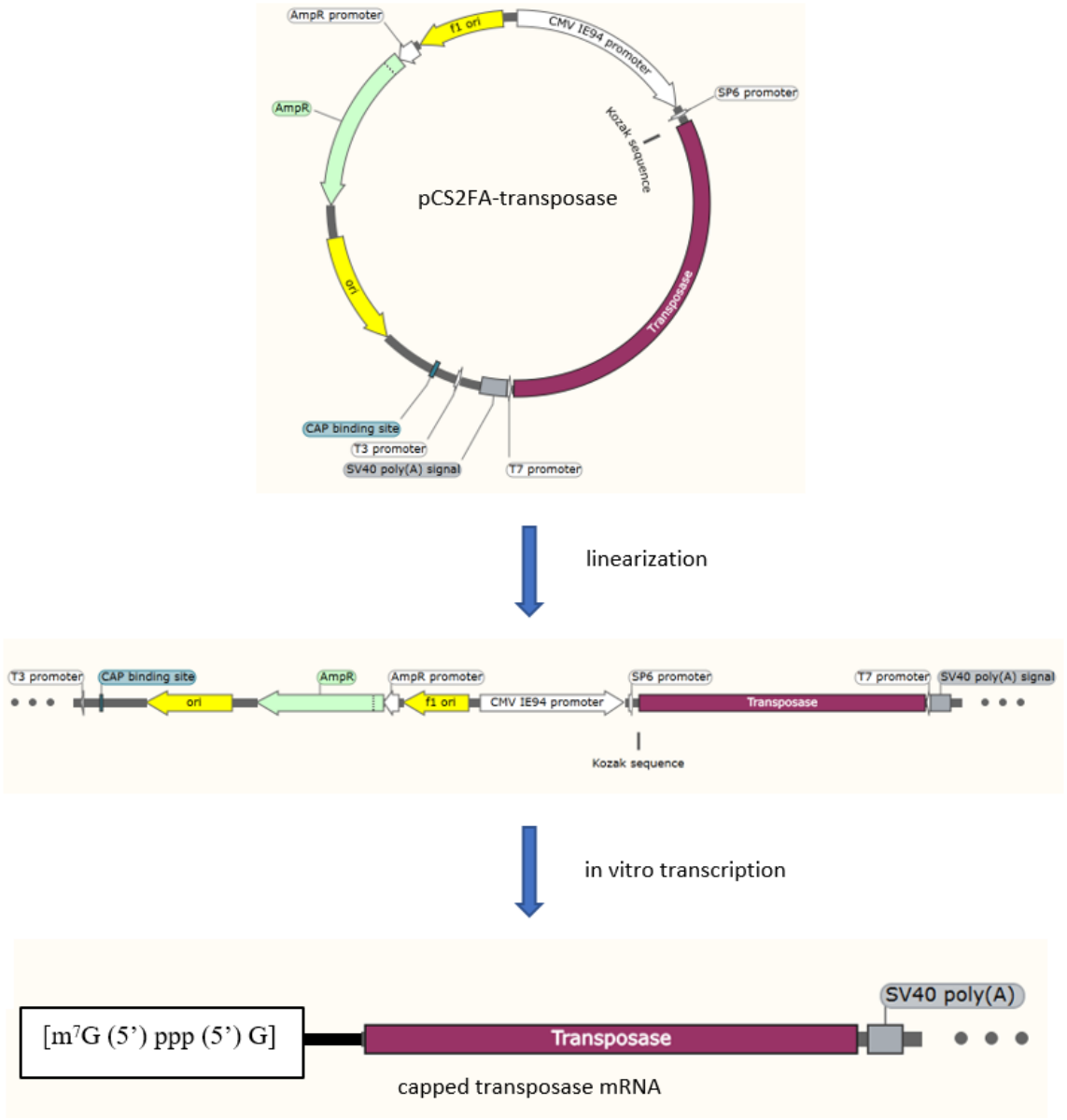

Figure 2.4 Tol2 transposase capped mRNA synthesis in vitro transcription.

The frozen reagents in table (Table 2.4.) was thaw on ice and reaction assembly was carried at room temperature. Mixture was gently mixed and spin down, then incubated at 37°C, 2 hours to achieve maximum yield. Recovery of the RNA was done by different methods such as Lithium chloride precipitation, Phenol:chloroform extraction and isopropanol precipitation or clean-up purification of a kit. Lithium chloride precipitation which is efficient to remove unincorporated nucleotides and most proteins is mostly used to precipitate RNAs smaller than 300 nucleotides. Phenol:chloroform extraction and isopropanol precipitation is the most rigorous method to purify mRNA, in which all enzyme and most of the free nucleotides are removed.

Table 2.4 In-vitro reaction set up.

Amount	Component
To 20 µl	Nuclease-free Water
10 µl	2X NTP/CAP
2 µl	10X Reaction Buffer
(1 µl)	(optional) [α-32P] UTP as a tracer
--	0.1–1 µg linear template DNA

2.7. Microinjection

Microinjection procedure is performed 20-30 minutes after fertilization of the eggs. Embryos are transferred to injection dishes which are prepared by 3% agarose gel and E3 medium. Eggs are aligned through the wells of the agarose gel. The plasmid and tol2 mRNA mix are injected directly to the cell of one cell stage embryos. Injection should be done 1-4 cell stage to guarantee that cell uptake and the mix is evenly distributed to the daughter cells. 1.0 mm OD glass capillary needles used for injection are prepared by a micropipette puller. Then, mix is loaded to the capillary needle by microloader pipette. The mix must be loaded carefully to keep the bubble formation at minimum while loading the needle. Needle is inserted to micromanipulator and with the help of a forceps tip of the needle is trimmed so that needle can easily penetrate through the chorion, yolk and blastomeres without giving any harm. Injection volumes are dependent on the region where injections are performed, which is generally between 500 pL to 1 nL. For efficient integration, the amount of construct along with *Tol2* transposase mRNA injected should be around 25 picograms. Thus, injection material is prepared as 25 ng/µl final concentration. Phenol red is mixed to injection material to confirm that the injection is performed on the right place.

2.8. Fin Resection

Zebrafish of 4-6 months age were used for all melanocyte ablation studies. Firstly, fish were anesthetized by Tricaine. Once fish were immobilized, the caudal fin of each fish were resected with razor blade. Four animals were used for each stage. Razor blade was sterilized after each resection to prevent cross-contamination. The dorsoventral resection was performed at half of the caudal fin to obtain maximum content without disrupting the regeneration potential

of the fin. For melanoma models, tumors that developed on fin (caudal, dorsal, anal) were resected from fish to constitute a significant sampling with regeneration models of fin melanocytes.

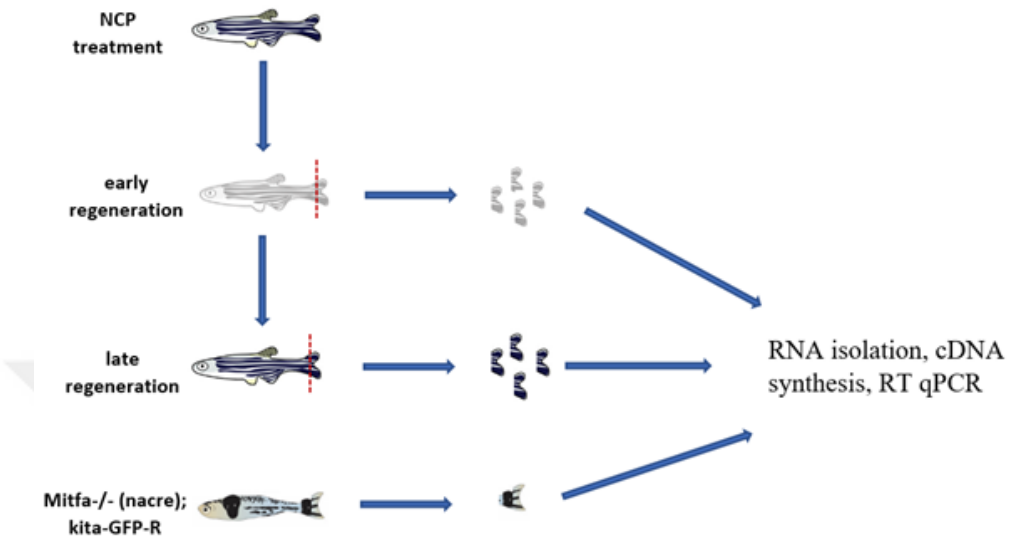

Figure 2.5 Sampling plan of regeneration and melanoma models of zebrafish. Following NCP treatment, caudal fin resected from the early and late melanocyte regeneration models. Four individuals were sampled for each regeneration group. Melanoma resection was done primarily from dorsal, anal and caudal fin of individual fish.

2.9. RNA Isolation

RNA isolation was carried out by RNeasy® Micro Handbook (QIAGEN). Fins were placed into QIAzol Lysis Reagent and immediately proceeded to tissue disruption and homogenization. If QIAzol procedure was not applied right after fin cut, fins were submerged in RNA Stabilization Reagent that preserves the gene expression pattern and stabilizes cellular RNA in situ. According to RNeasy® Micro Handbook (QIAGEN), tissue weight more than 5 mg exceeds binding capacity of RNeasy MinElute spin column and lowers the yield. Fins were weighted to determine the amount and it was confirmed that starting material was suitable for kits requirements. Tissue disruption was performed with pestle (Fisherbrand RNase-free disposable pestles). Then, lysate was passed through insulin needle (20-gauge, 0.9 mm) at least 5-10 times to achieve proper homogenization. The whole protocol as in the following:

Tissue was homogenized in 700 µl QIAzol reagent. 140 µl Chloroform was added to homogenate. Homogenate was shaken vigorously 15 s and was incubated at RT for 2-3 minutes. Then, homogenate was centrifuged at 12,000 x g for 15 min at 4°C, in which 3 phases were separated. The upper phase containing RNA was transferred to 1.5 mL microcentrifuge tube. 1

volume of 70% ethanol (prepared with DEPC water) was added and mixed thoroughly by vortexing. The mixture was transferred to RNeasy MinElute spin column. The procedure "Appendix C: RNA Cleanup after Lysis and Homogenization with QIAzol Lysis Reagent" in RNeasy® Micro Handbook was performed for the following steps. All centrifugation steps were performed at 20–25°C in a standard microcentrifuge at 15.000 rpm. DNAse I treatment was considered necessary because RNA samples would be very sensitive to contamination of genomic DNA for qPCR. After all, washing steps were applied, the RNeasy MinElute spin column was placed in a new 1.5 ml collection and 14 µl RNase-free water was added directly to the center of the spin column membrane. Tubes were centrifuged for 1 min at full speed to elute the RNA. Total RNA concentration was determined using 1 µl of sample by NanoDrop™ 2000/c Spectrophotometers (Thermo Fisher Scientific). RNA quality was verified on Agilent RNA 6000 Pico kit according to manufacturer's instructions using 1 µL of a 1:100 dilution in H_2O of each purified total RNA sample in order to confirm that RIN scores were above 7.0.

2.10. cDNA Synthesis and qPCR

cDNA synthesis was performed from the RNA samples by using iScriptTM cDNA synthesis kit (BIORAD). Reaction set up in Table 2.5:

Table 2.5 cDNA synthesis reaction set up

Component	Volume per reaction, µl
5X iScript Reaction Mix	4 µl
iScript Reverse Transcriptase	1 µl
RNA Template (1µg)	variable
Nuclease free water	variable
Total volume	20 µl

qPCR reactions were set up by using GoTaq® qPCR Master Mix (Promega) kit in Table 2.6. 2X Master Mix includes all reagents required for qPCR reaction, such as polymerase, $MgCl_2$, dNTPs, ds-DNA binding dye and buffer. cDNAs (1 µg) were diluted as 1:30 in nuclease free water. Appropriate amounts of reaction mix were added to wells, then DNAs were distributed (Fig. 2.6). Reaction plate was sealed and centrifuged at 1000 rpm for 2 minutes to eliminate bubbles.

Table 2.6 qPCR reaction set up

Components	Volume per 10 µl reaction	Final concentration
Master Mix, 2X	5	1X
Nuclease-Free Water	0	
qPCR primers (10µM)	1	1µM
cDNA template	4	

Applied Biosystems® 7500 Real-Time PCR thermal cycler was programmed as the manufacturer‘s instructions; SYBR® detection dye was selected, ROX™ was selected as reference dye, standard (2 hours) program was selected.

Table 2.7 Primers used in qPCR

Sequence (5'->3')	
Endogenous control	
rpl13	
Forward primer	CCCTCCACCTTATGACAAGAGA
Reverse primer	CGTCCAAGCAGGGCAAATTT
product length	96
Proliferation marker	
pcna	
Forward primer	CAAGGAGGATGAAGCGGTAACA
Reverse primer	CTGCGGACATGCTAAGTGTG
Product length	128
Melanocyte development/regeneration markers	
mitfa	
Forward primer	ACCTGATGGCTTTCCAGTAGAAG
Reverse primer	TGCTTTCAGGATGGTGCCTTT
Product length	190
tyr	
Forward primer	TAATCCTGAGACGGGTTTGGC
Reverse primer	CACTGCTCAAAGATGCTGTCAAT
Product length	156
tryp1a	
Forward primer	GAACTCCATCGAGGGCTACAG
Reverse primer	GGAATATGGGGTCGTTGGGG
Product length	134
dct	

Forward primer	AGACGCTTCCGTGAAAACGA
Reverse primer	CTGTTGTCCAGTTCTTCGAGGT
Product length	170
tyrp1b	
Forward primer	TTTGCTATTGGAGGCAGCGA
Reverse primer	GGACTGGATTCTGTGTTGTTGC
Product length	179
Cancer marker	
fosab	
Forward primer	CCCGAGCTCTTACCCCAAAAT
Reverse primer	CTGGTCAGTTTCAGCTTGCAG
p21	
Forward primer	ACTTCCAGCTTCAGGTGTTCC
Reverse primer	CGGCCCATTACCGAGTGAA
dusp6	
Forward primer	GAGATGCAAGACGGACACGA
Reverse primer	ATTTGCTGAAGCCACCCTCG
Melanocyte/Neural crest stem cell marker	
crestin	
Forward primer	AGTGCCTGCCAATGTTCAC
Reverse primer	CTGAAAAAGGCCGATGAGTT
sox10	
Forward primer	ATATCCGCACCTGCACAA
Reverse primer	CGTTCAGCAGTCTCCACAG
dlx2a	
Forward primer	ATCTCTGGGCCTCACGCAAA
Reverse primer	GGGTGGGATCTCTCCACTTTT
Xanthaphore development/regeneration marker	
xdh	
Forward primer	GGCTTAGGTCTGTTCACGCT
Reverse primer	GAGGTTCACCCACAGCCTTT
csf1ra	
Forward primer	AGTCCGTATCCAAACATCCTGG
Reverse primer	GGCTGATCTTGCTGAATGTGG

Standard curves were plotted by the standard curve analysis section of by Applied Biosystems 7500/7500 Fast. Firstly, serial dilutions of cDNA template were prepared as 1:5, 1:25, 1:125 and 1:625. Serial dilutions were used in separate real-time reactions for each primer. The software plotted a standard curve from the C_T values of each reaction and correlation

coefficient (R_2) of each primer was deducted from the plot. The R_2 values 0.99 or greater were used in the qPCR reactions.

2.11. Histology

Fish were killed by immersion in Tricaine (Sigma-Aldrich). After decalcification procedure fish were dissected in half transversely to increase penetration of fixative. Fish were fixed in 10% Formaldehyde for 3 days at RT, washed once with PBS and decalcified in 0.5 M EDTA pH 8 for 5 days at 4°C. Paraffin embedding procedure as in the Table 2.8. Tissue samples were sectioned as 5 µm thickness.

Table 2.8 Paraffin embedding procedure performed for whole zebrafish.

	Time	Temperature
70 % Alcohol	1 hour	RT
80 % Alcohol	1 hour	RT
96 % Alcohol	1 hour	RT
100 % Alcohol	1 hour	RT
100 % Xylene	1 hour	60°C
100 % Xylene	1 hour	60°C
Paraffin	1 hour	60°C
Paraffin	1 hour	60°C

2.12. Hematoxylin and Eosin Staining

Hematoxylin and Eosin Staining (H&E) is commonly used to stain melanoma samples. Basophilic structures like nuclei are stained blue whereas eosinophilic structures like membrane are stained pink. Sections obtained from paraffin embedded requires following rehydration and washing steps to deparaffinate the sample slide; wash in Xylene for 2 X 2-minutes, wash in absolute Ethanol for 2 minutes, wash in Ethanol 95% for 2 minutes, wash in Ethanol 70% for 2 minutes, wash in Ethanol 50% for 2 minutes, wash in Ethanol 50% for 1 minutes. Right after deparaffination, the following steps were performed for hematoxylin and eosin stain of sections; incubate in Hematoxylin 5 minutes, immerse in acid alcohol immediately, immerse in Eosin for 2 minutes, immerse in ethanol 95% immediately for 30 seconds, wash in absolute ethanol

for 3X2 minutes, wash in xylene 3 X 5 minutes. Slides were mounted Entellan right after staining steps and covered.

2.13. Materials

Following figure shows the zebrafish lines used in this study. chemicals and machines used in this study (Table 2.9, Table 2.10).

Zebrafish lines	Alleles	Mutations	Phenotype
AB			Wild type
casper	Mitfa-/-: roy-/-	*mpv17*^{a9}*; mitfa*^{w2}	Lacks melanocytes and iridophores
nacre	*mitfa-/-*	*nac*^{w2}	Lacks melanocytes
Clementine	*mitfa-/-* (*nacre*); *kita*:GFP-RAS^{G12V}	*nac*^{w2}	Lacks melanocytes
ABXCle	mitf+/-		Wild type phenotype
ABXCle	*mitfa+/-* (*nacre*); *kita*:GFP-RAS^{G12V}	*nac*^{w2}	Lack melanocytes, RAS under *kita* promoter

Figure 2.6 Transgenics and mutants used in this study.

Following table shows the chemicals and devices used in this study.

Table 2.9 List of catalog numbers and brands of the chemicals.

Chemicals		
Ethanol	K45636683426	Merck
Yeast Extract, Bacteriological	J850-500G	Amresco
Ultrapure Agarose 500 g	16500-500	Invitrogen
Tricaine	A5040-25g	Sigma
Phenol Red, powder	P3532-5g	Sigma
2-propanol	K45187334402	Merck
Agar	VM623914347	Merck
Paraformaldehyde (1 kg)	K45535705424	Merck
Potassium Chloride	K45117936405	Merck
Tryptone	J859-500G	Amresco
Chloroform	1.02431.2500	Merck
Eosin Y-Solution %5 Aqueous	1.09844.1000	Merck
Eosin Y-Solution Alcoholic (500ML)	HT110116-	Sigma
Entellan (100 ml)	1.07961.0100	Merck
Teksoll 96 (5L)	TK.200650.05001	Tekkim

Ethanol Absolute (2,5L)	1.00986.2500	Merck
Methanol	32213-2,5L	Sigma
Paraformaldehyde (1 kg)	1.04005.1000	Merck
Paraffin (C pure) (1 kg)	TK.200660.01000	Tekkim
Xylenes	16466-2,5L	Sigma
DEPC (Diethylpyrocarbonate) (100 ML)	D-340-100	Gold Bio
Ethidium bromide (10 ml)	ETB444.1	Bioshop
Phenol Red	P3532-5G	Sigma
S.O.C. Medium	15544-034	İnvitrogen
Agar	1.01614.1000	Merck
Agorose LE	A-201-100	GoldBio
D - (+) - Glucose Monohydrate	16301-1KG	Sigma
Edta Disodıum Salt Dihydrate	0105-1KG	Amresco
Glycerol	0854-1L	Amresco
Neocuproine	N1501-5G	Sigma
Potassium Chloride	1.04936.1000	Merck
Potassium Phosphate Monobasic 500 g	PPM666.500	Bioshop
Sodium Chloride (5 kg)	1.06400.5000	Merck
TRIS	0826_1KG	Amresco
Yeast Extract Granulated (500 g)	1.03753.0500	Merck
Mayer's Hematoxylin Solution	MHS16-500ML	Sigma
Chloroform	1.02431.2500	Merck
Paraformaldehyde (1 kg)	1.04005.1000	Merck
Parafin (C pure) (1 kg)	TK.200660.01000	Tekkim
Xylenes	16466-2,5L	Sigma

Table 2.10 List of brands of the devices.

Devices	
Basic power supply	Biorad
Universal Power Supply	Biorad
mySPIN™ 6 Mini Centrifuge	Thermo
Water bath and Lid	Nüve
PH Meter	Hanna
Microwave oven	Beko
Basic PCR	Life Sciences
Balance - basic	Sartorius
Vortex Mixer	Thermo
Stemi 305 Compact Stereo Microscope	Zeiss
SZX2 Series stereo microscope	Olympus
StabiliTherm™ Ovens and Incubators	Thermo
Dry Bath Incubator	Allsheng
SimpliAmp Thermal Cycler	Applied Biosystems
Borosilicate glass capillary	World Precision Instrument

Flaming/Brown Micropipette Puller	Sutter Instrument
Pasteur pipette glass 145 mm	Isolab
Filter tips (10 µl, 20 µl, 200 µl, 1000 µl)	Vertex
PV820/PV830 Pneumatic Picopump	World Precision Instrument
MicroCL 17 Microcentrifuge	Thermo
Mikro 200 Centrifuge	Hettich
Applied Biosystems 7500/7500 Fast	Applied Biosystems

RESULTS

3.1. NCP Treatment Ablated Zebrafish Melanocytes

We performed 1-day NCP treatments to see the pattern of depigmentation and to decide early and late melanocyte regeneration stages. Firstly, we treated 4-months-old wild type (AB) line with NCP for 24 hours. We imaged the regeneration process day by day to observe melanocyte death, to catch the time of exact melanocytes disposal out of skin, onset of melanocyte differentiation and the completion of regeneration process. Figure 3.1 shows the depigmentation and regeneration process of 1-day NCP treated fish. Here, we followed up the morphology of melanocytes till most of all the melanin content is cleared. We observed that fish slightly started to lose melanocytic aggregates on body at 3 dpa (not shown). The first cumulative loss of melanocyte aggregates appeared on the body at 4 dpa in which fish mostly devoid of melanin pigmentation throughout the black stripe. Some melanocytic aggregates were not disposed out of fin and remained as black smear through the black stripe of fin. Even though melanocyte aggregates are not extruded out of the fin they totally lost their dendritic morphologies and display a smear of scattered black aggregates. In this stage we can say that melanocytes lost all cellular activities. At 7 dpa, regenerating melanocytes start to differentiate and appear throughout the body. Melanocyte regeneration and reconstitution of stripe pattern were established within 15 day after we returned fish to fresh water.

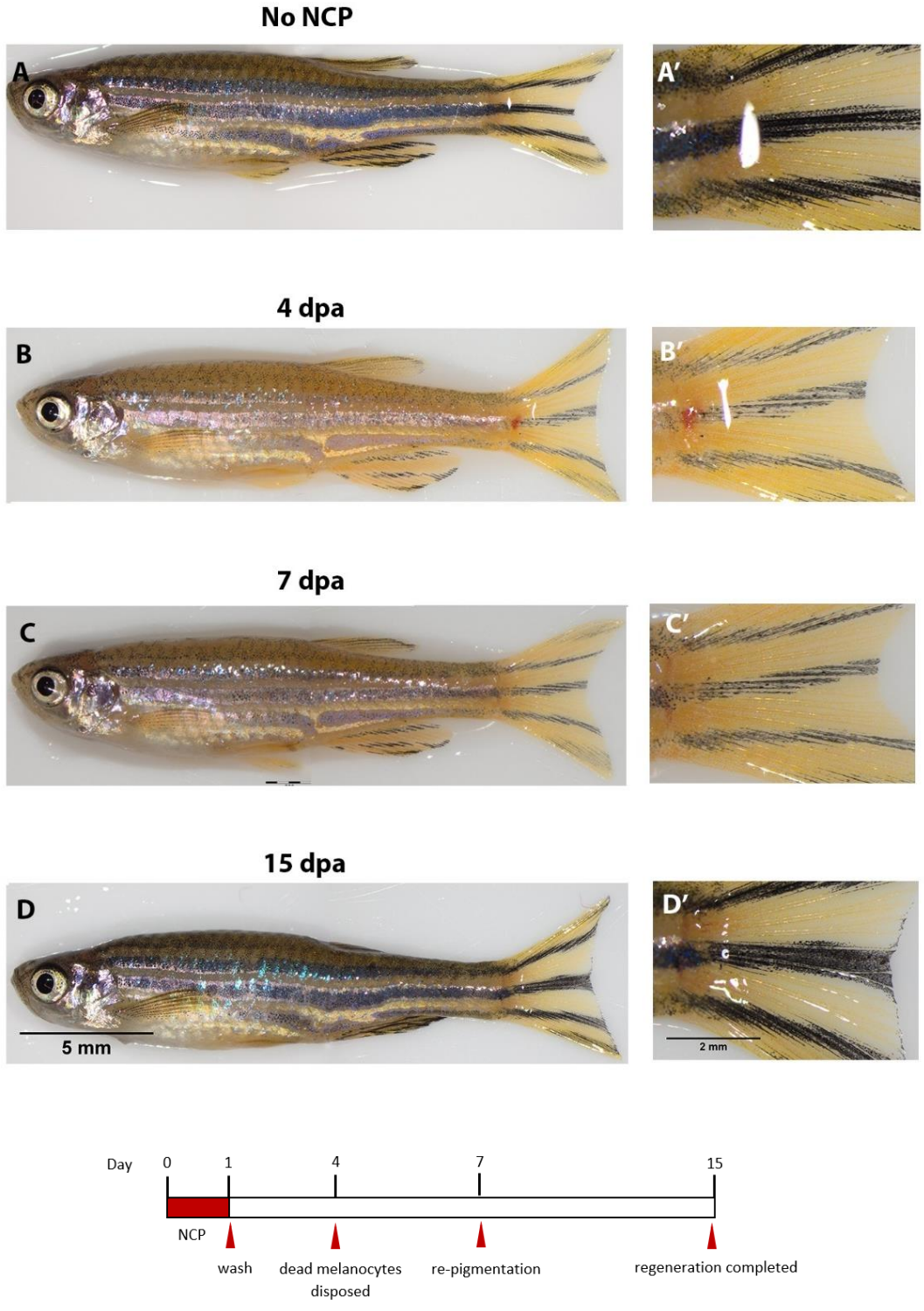

Figure 3.1 One-day of NCP treated Zebrafish melanocyte regeneration and reconstitution of stripe pattern for 15 days. (A) Zebrafish at 0 day is untreated with normal stripe pattern on body and fins. **(B)** At 4 dpa melanocytes were totally extruded out of the skin. Stripe pattern is not visible anymore However, complete extrusion was not achieved out of fin. **(C)** At 7 dpa melanocytes slightly appeared along the body and fin**. (D)** At 15 dpa melanocyte regeneration was completed and stripe pattern was established. **(A'-D')** Close-ups of fin of each fish. Scale bars in **(A-E)** are 5 mm and in **(A'-D')** are 2 mm.

We were next interested whether NCP kills almost all melanocytes on fin. We performed epinephrine treatments on control group and on fish at 1 dpa and 2 dpa. We observed that melanocytes showed immediate response to epinephrine in the fin of untreated animals. The dendritic morphology of melanocytes turned into compact rounds showing that epinephrine treatment leads to aggregation of melanin towards the nucleus (Fig. 3.2A-A'). On the other hand, we did not observe remarkable contraction of melanocytes at 1 dpa. Although the shape of the melanocytes still is dendritic at 1 dpa, melanocytes could not respond to epinephrine (Fig. 3.2B-B). On 2 dpa, we observed the scattered smear of residual melanocytic aggregates on fin with no longer dendritic shaped and no response to epinephrine (Fig. 3.2C-C'). We conducted 1-day NCP treatments and demonstrated that after 24 hours of treatment melanocytes on body and fin are dead.

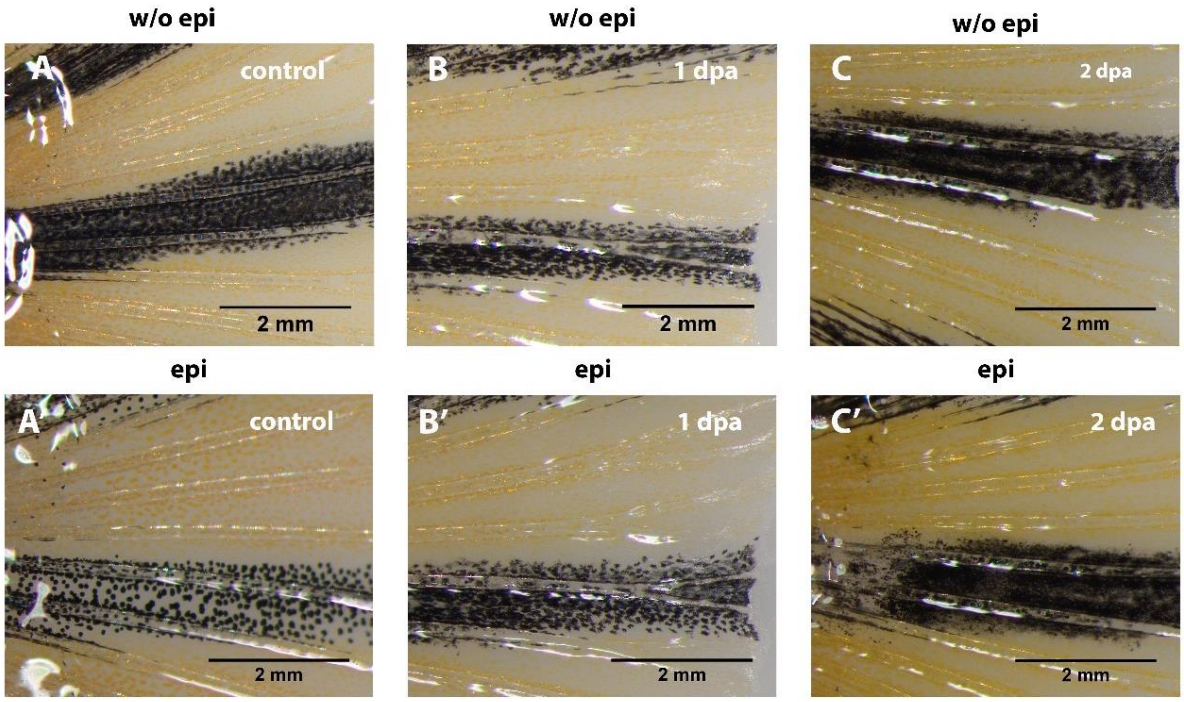

Figure 3.2 Epinephrine treatment of untreated and NCP treated fish. (A) Caudal fin of control fish that was not treated with epinephrine**. (A')** Control fish treated with epinephrine responded to epinephrine by losing dendritic appearance by gathering melanosomes around nucleus. **(B)** Fin of 1-day NCP treated fish at 1 dpa. **(B')** Fin of 1-day NCP treated fish under the epinephrine stimulation at 1 dpa. **(C)** Fin of 2-day NCP treated fish at two dpa. **(C')** Fin of 2-day NCP treated fish under the epinephrine stimulation at 2 dpa. Epinephrine caused immediate response in control fish, but not in NCP treated dish at 1 dpa and 2 dpa. Even though at 1 dpa melanocytes seem to be intact, they are dead and unable to respond epinephrine. At two dpa, there are no anymore melanocyte shaped structures instead a black smear spans the fin. Scale bars in **(A-C)** and in **(A'-C')** are 5 mm.

3.2. Early and Late Melanocyte Regeneration Stages Were Determined

Successful melanocyte ablation paved the way for us to decide early and late melanocyte regeneration stages. We exploited 4-month old wild type (AB) in our melanocyte regeneration studies and the previous methodology was applied to ablate melanocytes. We then cut fins at 4 dpa, 7 dpa, 12 dpa, 15 dpa and 20 dpa fins and performed immediately RNA isolations. We pooled 4 fin fish for each group. In our qPCR analysis, we used proliferation marker *pcna* as early marker of melanocyte regeneration. We found that *pcna* expression was nearly 1.5-fold higher at 4, 7, 12 dpa when compared to WT (Fig. 3.3A). We also checked *mitf* as early melanocyte development/regeneration marker at 4, 7, and 12 dpa and found that *mitf* had the highest expression at 4 dpa whereas at 7 and 12 dpa its expression fell down to control level (Fig. 3.3B).

Here we additionally checked for melanocyte differentiation markers of *dct*, *tyr*, *tyrp1a* and *tyrp1b* for late melanocyte regeneration/differentiation. All the differentiation markers showed reasonable similar pattern of expression through the days, in which all had the highest expression level at 7 dpa; 6-fold increased expression of *tyr*, *tyrp1a* and *dct*; 3-fold *tryp1b*. Then, accordantly all the expressions fell down to control level. Even though we found that expression of differentiation markers was highest at 7 dpa, their expression showed significant increase even at 4 dpa in which expression of early regeneration marker *pcna* was still high (Fig. 3.3 C-F). Thus, we can say that late regeneration of melanocytes is established at 7 dpa. However, the increase of late regeneration markers at 4 dpa indicates that early regeneration should be before the 4 dpa.

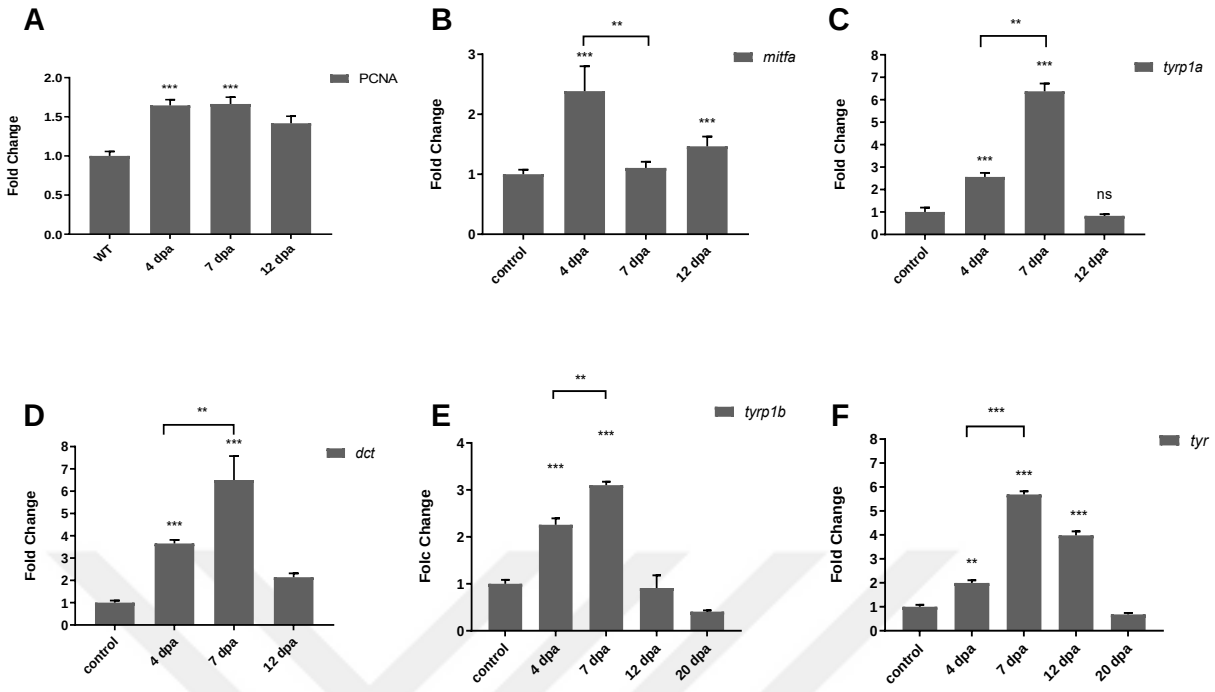

Figure 3.3 Real-time PCR analysis of mRNAs of *mitfa, dct, tyr, tyrp1a* and *tyrp1b* for the control and NCP treated animal groups. *rpl13* was used as endogenous control. Relative mRNA level was normalized to the corresponding *rpl13* mRNA expression. qPCR data presented here are means ± SD from triplicate data. Asterisk on individual bars represents significant difference between control group and NCP groups. Asterisks on half tick-up lines represents significant difference between the indicated groups. Student's unpaired t test was used to calculate significance *P < 0.05, **P < 0.01, ***P < 0.001. Error bars indicate SEM. Data represented here compares the expression levels of **(A)** *pcna* between control, 4 dpa, 7 dpa and 12 dpa groups (4 dpa P= 0.0003, 7 dpa P= 0.0002, 12 dpa P= 0.0003). **(B)** *mitfa* between control, 4 dpa, 7 dpa and 12 dpa groups (4 dpa P= 0.0008, 7 dpa P= 0.0668, 12 dpa, P= 0.0010, 4 dpa versus 7 dpa, P=0.0017). **(C)** *tryp1a* between control, 4 dpa, 7 dpa and 12 dpa groups (4 dpa P= 0.0060, 7 dpa P= 0.0002, 12 dpa P= 0.3429, 4 dpa versus 7 dpa, P= 0.0066). **(D)** *dct* between control, 4 dpa, 7 dpa and 12 dpa groups (4 dpa P= <0.0001, 7 dpa P= <0.0001, 12 dpa P= <0.0001, 4 dpa versus 7 dpa, P= 0.0015). **(E)** *tyrp1b* between control, 4 dpa, 7 dpa, 12 dpa and 20 dpa groups (4 dpa P= 0.0001, 7 dpa P= <0.0001, 12 dpa P= 0.5232, 20 dpa P= <0.0001, 4 dpa versus 7 dpa, P= 0.0048). **(F)** *tyr* between control, 4 dpa, 7 dpa, 12 dpa and 20 dpa groups (4 dpa P= 0.0015, 7 dpa P= <0.0001, 12 dpa P= 0.0002, 20 dpa P= <0.0001, 4 dpa versus 7 dpa, P= 0.0048).

Assessing that early regeneration should be before 4 dpa, we collected fin at 1, 2, 3, 4 and 7 dpa. We checked *pcna*, *dct* and *tyr* markers by qPCR and found that *pcna* expression was highest at 1 dpa as nearly 2-fold increased expression when compared to control group. *pcna* expression decreased gradually until its expression was balanced with the control group at 7 dpa (Fig. 3.4A). We also analyzed that *tyr* and *dct* had the highest expression levels at 7 dpa (Fig. 3.4B-C). The expression levels were 8-fold and 3-fold at 7 dpa for *dct* and *tyr*, respectively. *dct* expression spontaneously increased at 3 dpa and kept its expression high until 7 dpa. We also treat *casper* mutant that is devoid of melanocytes with NCP for 24 hours. At 1 dpa and 2 dpa fin of four fish were clipped and pooled. *pcna* proliferation marker was checked at these

days to see whether proliferation mechanisms were triggered also in *casper*. However, any significant change was not found (Fig 3.4D).

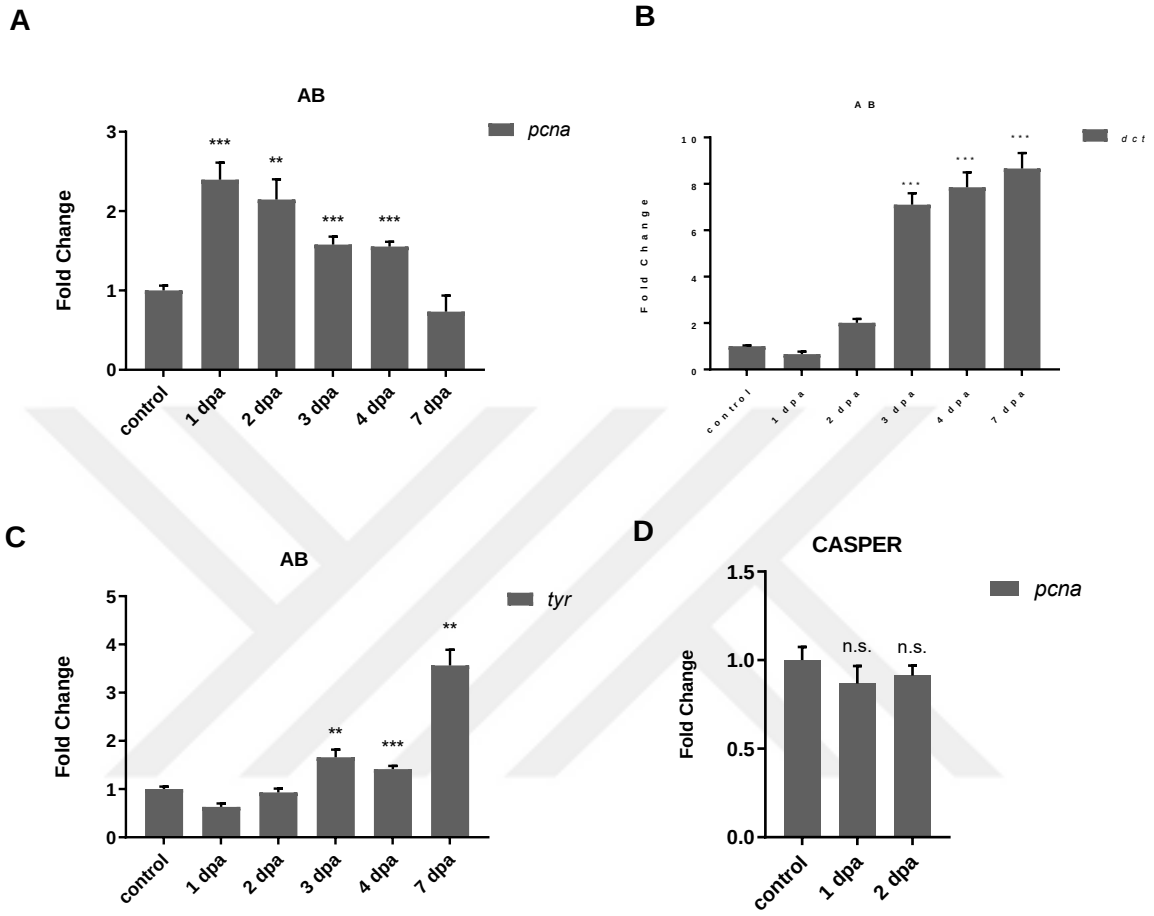

Figure 3.4 Real-time PCR analysis of mRNAs of *pcna*, *dct* and *tyr* for the control and NCP treated animal groups. *rpl13* was used as endogenous control. Relative mRNA level was normalized to the corresponding *rpl13* mRNA expression. qPCR data presented here are means ± SD from triplicate data. Asterisk on individual bars represents significant difference between control group and NCP groups. Asterisks on half tick-up lines represents significant difference between the indicated groups. Student's unpaired t test was used to calculate significance *P < 0.05, **P < 0.01. Error bars indicate SEM. Data represented here compares the expression levels of **(A)** *pcna* between control, 1 dpa, 2 dpa, 3 dpa, 4 dpa and 7 dpa (1 dpa P= <0,0001, 2 dpa P= 0,0042, 3 dpa P= 0,0001, 4 dpa P= 0,0003, 7 dpa P= 0,1280). **(B)** *dct* between control, 1 dpa, 2 dpa, 3 dpa, 4 dpa and 7 dpa (1 dpa P= 0,0042, 2 dpa P= 0,0004, 3 dpa P= <0,0001, 4 dpa P= <0,0001, 7 dpa P= <0,0001). **(C)** *tyr* between control, 1 dpa, 2 dpa, 3 dpa, 4 dpa and 7 dpa (1 dpa P= 0,0119, 2 dpa P= 0,0012, 3 dpa P= <0,0001, 4 dpa P= 0,0025, 7 dpa P= 0,0005). **(D)** *pcna* between CASPER control, 1 dpa and 2 dpa (1 dpa P= 0,1284, 2 dpa P= 0,1157).

In order to show that early and late regeneration pattern are the same at the individual level, we needed to perform the same procedure for individuals. We checked for *pcna* and *dct* markers at control, 1 dpa and 7 dpa (Fig. 3.5). We found the consistent results with the previous analysis in which at 1 dpa proliferation high (2.5-fold and 6-fold) and at 7 dpa proliferation fell down to control level.

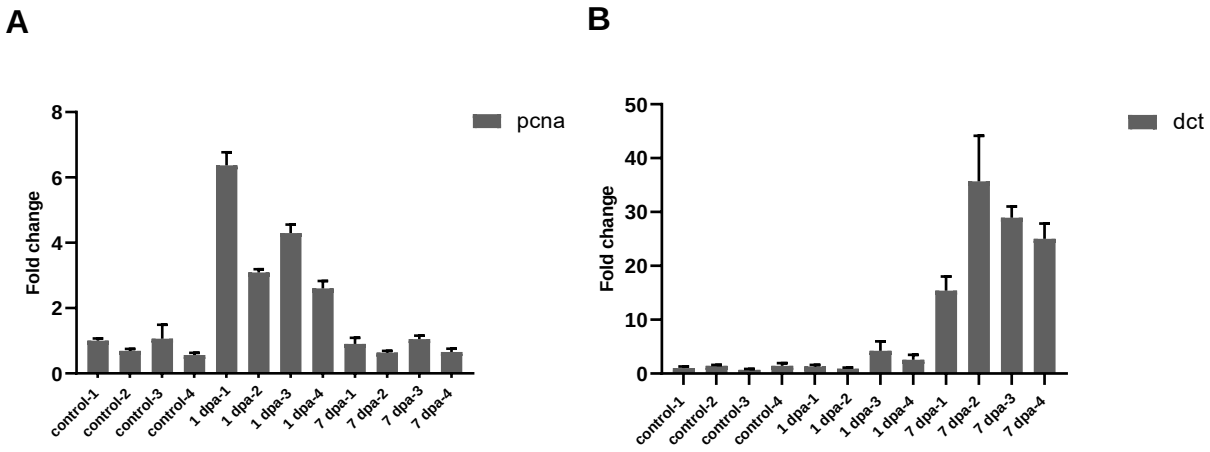

Figure 3.5 Real-time PCR analysis of individual mRNAs for *pcna* and *dct* for the control and NCP treated groups. *rpl13* was used as endogenous control. Relative mRNA level was normalized to the corresponding *rpl13* mRNA expression. qPCR data presented here are means ± SD from triplicate data. Data represented here compares the expression levels of **(A)** *pcna* between 4 individuals of control, 4 dpa, 7 dpa and 12 dpa groups. **(B)** *dct* between 4 individuals of control, 4 dpa, 7 dpa and 12 dpa groups.

3.3. Crossbreeds of Tg(*kita*:HRAS^{G12V}:GFP) and Wild Type Developed Melanoma

We crossed wild type zebrafish line (AB) and *mitf*-/-; *kita*:GFP-RAS^{G12V} to generate zebrafish melanoma model in which benign and malignant phenotypes has been observed. The pigmentation pattern of *mitf*+/-; *kita*:GFP-RAS^{G12V} larvae that show overexpression of RAS^{G12V} only in melanocytes was imaged at 3, 6, 10 and 13 dpf. Enhanced pigmentation and disrupted pattern of *mitf*+/-; *kita*:GFP-RAS^{G12V} larvae melanocytes were easily observed beginning from 3 dpf.

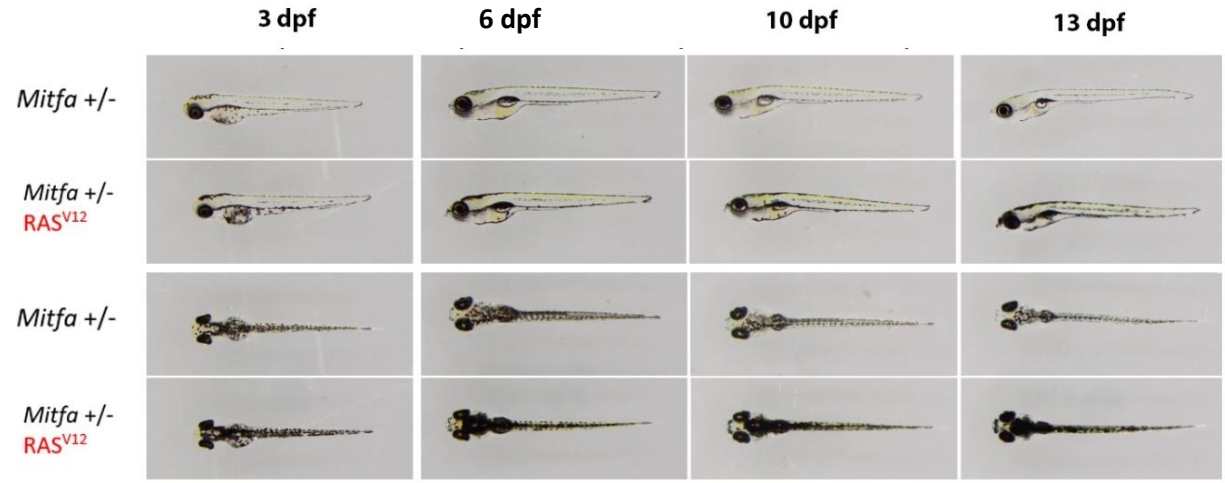

Figure 3.6 Expansion of *mitf*+/-; *kita*:GFP-RAS^{G12V} larvae melanocytes. m*itfa*+/- as control at 3, 6, 10 and 13 dpf. Side and dorsal views of larvae. The dorsal views of *kita*:GFP-RAS^{G12V} larvae displays disrupted pigment pattern.

In order to assess the ratio of melanoma transformation from melanocytic patches we counted melanoma growth at 4, 8- and 20-week post fertilization. All one moth old *mitf*+/-; *kita*:GFP-RAS^{G12V} fish developed only melanocytic hyperplasia that surrounds the body (mostly on dorsal parts) and disrupts stripe pattern. We did not observe melanoma growth among one-month old fish. However, approximately 17% of two months old fish (6 out of 36) developed melanoma growth and approximately 36% of two months old fish (4 out of 11) developed melanoma growth (Table 3.1). The tumor onset rate got high as the fish age.

Table 3.1 Melanoma scoring of adult *mitf*+/-; *kita*:GFP-RAS^{G12V} zebrafish

Week	Melanocyte expansion/ Melanocytic lesions	Melanoma growth	Total	Percent
4	41	0	41	
8	30	6	36	17%
20	7	4	11	36%

Superficial spreading *mitf*+/-; *kita*:GFP-RAS^{G12V} melanocyte expansion started to transform into melanoma growth in nearly 2 month. *mitf*+/- fish is shown as control in Figure 3.7A. 2 months old *mitf*+/-; *kita*:GFP-RAS^{G12V} fish developed small melanoma. In this stage melanoma has distinct borders. Ulceration and vascularization are not observed. Melanoma of 5-month-old fish on the hand have big mass of melanoma growth. Vascularization and ulceration are observed. The huge mass of melanoma caused deformation on the body. Fish in Figure 3.7D, have 4 distinct melanoma growth; on dorsal, dorsal fin, caudal fin and abdomen. Three of the melanoma growths are hyper-pigmented whereas the melanoma on dorsal side has hypo-pigmented nature. Fish in figure E, have only one huge melanoma growth on anal fin. The anal fin is disrupted because of mass growth. Melanoma of this fish has both hyper-pigmented and hypo-pigmented parts.

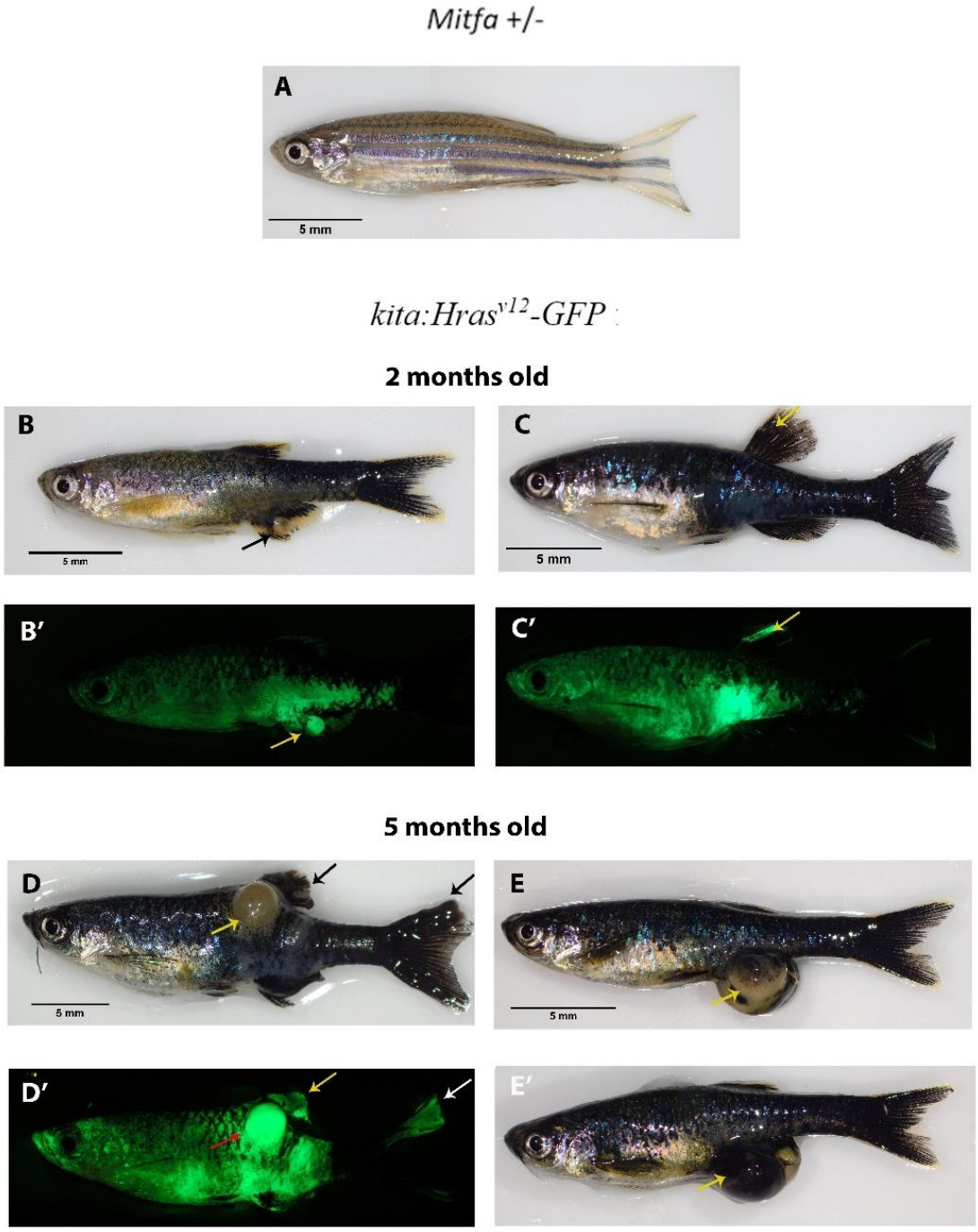

Figure 3.7 *mitf*+/-; *kita*:GFP-RAS^{G12V} develops tumor mostly on dorsal, dorsal fin, caudal fin and anal fin. **(A)** Mitfa+/- as control. **(B)** Two months old fish develops a small round melanoma on anal fin (black arrow). **(B')** Fluorescence image of the two months old fish, yellow arrow shows primer melanoma budding from the anal fin. **(C)** The left side of another two months old fish developed large melanoma bulk on anal fin. **(C')** The right side of the same fish. **(D)** Five months old fish developed tumor on dorsal back, on caudal fin and on dorsal fin. Tumor at dorsal is hypo-pigmented. Tumors at dorsal fin and caudal fin is hyper-pigmented. **(D')** Fluorescence image of the fish. Red arrow shows the hypo-pigmented tumor on dorsal. Yellow arrow indicating hype-pigmented tumor on dorsal fin. White arrow showing the hyper-pigmented tumor on fin. **(E)** Five months old fish developed hyper-pigmented growth on dorsal fin, yellow arrow. **(E')** Fluorescence image of the same fish. Scale bars in **(A-D)** are 5 mm.

3.4. Histologic Sections Showed *kita*:HRAS^{G12V} Induced Melanoma Display Progressed Malignancy

We chose 5-month-old control and *mitf*+/-; *kita*:GFP-RAS^{G12V} fish that has advanced melanoma for histological sectioning and performed H&E staining in order to assess whether the tumor display invasive characteristics. We performed formaldehyde fixation and paraffin embedding. The fish we chose had severe melanoma growth above the skin on the dorsal side and on dorsal fin (Figure 3.8 A-A'). The GFP signal strong in the regions that has mass growth. Melanoma cells were infiltrating various tissues including muscle and spinal cord. The melanocyte population is denser beneath the epidermis, between the basal membrane and stratum compactum of *mitf*+/-; *kita*:GFP-RAS^{G12V} fish compared to control fish skin. Histological sections showed that melanoma had both endophytic (going inward) and exophytic (going outward) growth pattern. Endophytic growth pattern led melanoma cells to spread through the muscle fascicles that surround the spinal cord and degenerate muscle bundles. The melanoma is not well circumscribed; it has irregular and infiltrative growth pattern towards to internal organs including muscle, kidney and spinal cord. The melanoma is mainly composed of epithelioid shaped cells.

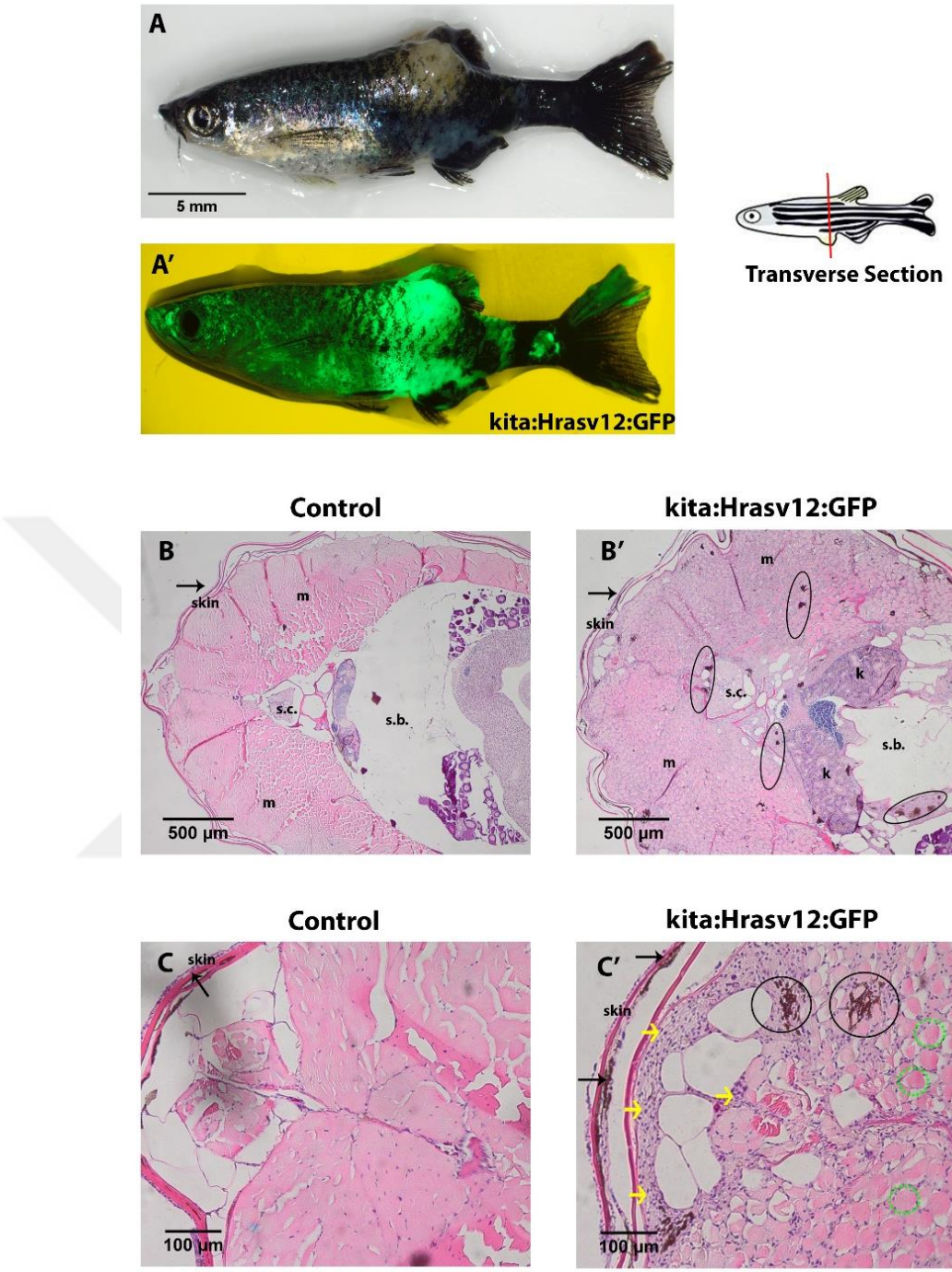

Figure 3.8 The H&A staining transverse sections of the paraffin embedded *mitf*+/-; *kita*:GFP-RAS^{G12V} and control fish. The stereo **(A)** and fluorescence **(A')** images of the fish sectioned. The sections of control **(B)** and *mitf*+/-; *kita*:GFP-RAS^{G12V} (B'). The close-up sections of control **(C)** and mitfa+/-; *kita*:Hras^{G12V}:GFP **(C').** Black arrow indicates the zebrafish skin. Spinal cord, muscle, kidney and bladder are indicated on the image (k, kidney; m, muscle; sc, spinal column; sb, swim bladder). Calibration bars for **A-A'**= 500 µm, for **B-B'**= 100 µm. Yellow arrows indicate the melanoma cells that is composed predominantly of epithelioid shaped cells. Black circles show the melanoma cell infiltrations to spinal cord, muscle, kidney and ventral structures. Dashed green circles show degenerated muscles bundle**.**

3.5. MiniCoopR Injections to *mitfa*-/-; *roy*-/-; *p53*+/-; RAS^{G12V} Led Hyperproliferation of Rescued Melanocytes

We showed that *mitf*+/-; *kita*:GFP-RAS^{G12V} line developed melanoma in two months. However, we wanted to accelerate the melanoma onset and thought that *p53*+/- background might help melanoma initiation in faster and aggressive manner. Therefore, we cloned required elements into MiniCoopR and formed an expression clone. Then we injected this clone into 1 cell-stage embryo of *mitf*-/-;*roy*-/-; *p53*+/-; RAS^{G12V} which is obtained through two backcrosses of *mitfa*-/-; *kita*:GFP-RAS^{G12V} to *casper* and *p53*-/- mutant. We imaged uninjected and injected embryo at 1 dpf, 3 dpf and 10 dpf. At 10 dpf we compared injected larva with WT larva because uninjected *mitfa*-/-; *kita*:GFP-RAS^{G12V} is devoid of melanocyte development due to *mitf* knockout.

GFP signal in Figure 3.9A represent *mitf* expression at 1 dpf of embryo. *mitf* expression is scattered throughout the body of embryo mostly on dorsal ridge and head parts. At 3 dpf *mitf* expression is restricted to melanoblasts (melanocyte stem cells) and melanocytes (Fig. 3.9 B-B', C-C'). Figure 3.9D shows AB-WT and MiniCoopR injected *mitfa*-/-; *kita*:GFP-RAS^{G12V} larva. We observed that overexpression of mutant RAS led altered pigmentation in which all head and body melanocytes are over expand and individual melanocytes grew larger comparing to control larva.

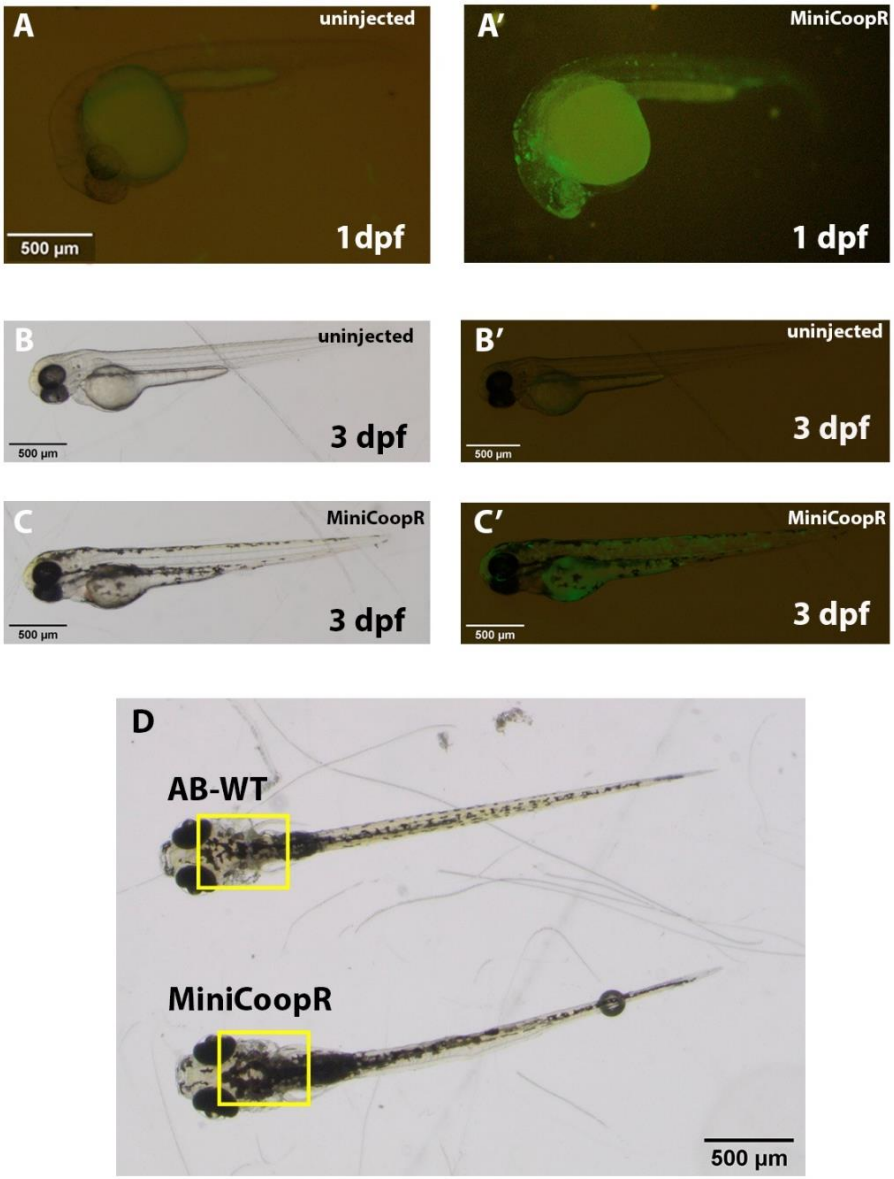

Figure 3.9 Phenotype of miniCoopR injected *mitfa*-/-; *roy*-/-; *p53*+/-; RAS^{G12V} embryo at 1 dpf, 3 dpf and 10 dpf. (A) fluorescence image of uninjected ***mitfa*-/-; *kita:*RAS^{G12V}** at 1 dpa **(A')** fluorescence image of MiniCoopR injected embryo at 1 dpf with GFP signal all distributed through the body especially on the dorsal and head structures **(B)** uninjected embryo at 3 dpa devoid of melanocyte development **(B')** MiniCoopR injected embryo at 3 dpa with melanocytes on dorsal, head and yolk. **(C)** fluorescence image of uninjected embryo at 3 dpa **(C')** fluorescence image of MiniCoopR injected embryo at 3 dpa **(D)** AB-WT vs MiniCoopR injected *mitfa*-/-; *roy*-/-; *p53*+/-; RAS^{G12V} embryo at 10 dpa. Yellow squares are spanning the head regions. MinicoopR injected larva displaying melanocyte overexpansion and larger sizes.

3.6. Late Melanocyte Regeneration Identity Is Related to Pigmented Melanoma Whereas NCC Identity Is Related to Unpigmented Melanoma

Here we used *mitf*+/-; *kita*:GFP-RAS^{G12V} melanoma models in qPCR analysis. We excised tumor formed on the caudal and anal fin since we performed our regeneration experiment on fish fin. RNAs harvested from fin would constitute more significant data for

qPCR analysis and for the future experiments. Similarly, control groups were chosen from caudal and anal fin of the healthy animals (mitf+/-). RNA isolation was performed with kit because regeneration experiments were carried out with RNA isolation kit. Besides, some of the tumors have small sizes and we did not want to lose any of the RNA content. Then we checked for *pcna*, *mitfa*, *tyr*, *dct*, *dusp6*, *p21* and *fosab* for the control and hyper-pigmented melanoma developed on caudal fin. qPCR data showed that hyper-pigmented tumor formed on caudal fin had differentiated state of melanocyte since the expression of *tyr*, *mitf*, and dct expression is high (Figure 3.10-3.11). *dusp6* (RAS target), *p21* (pI3K/AKT target), *fosab* (Erk/MAPK target) markers were checked for tumor identity altered pathways.

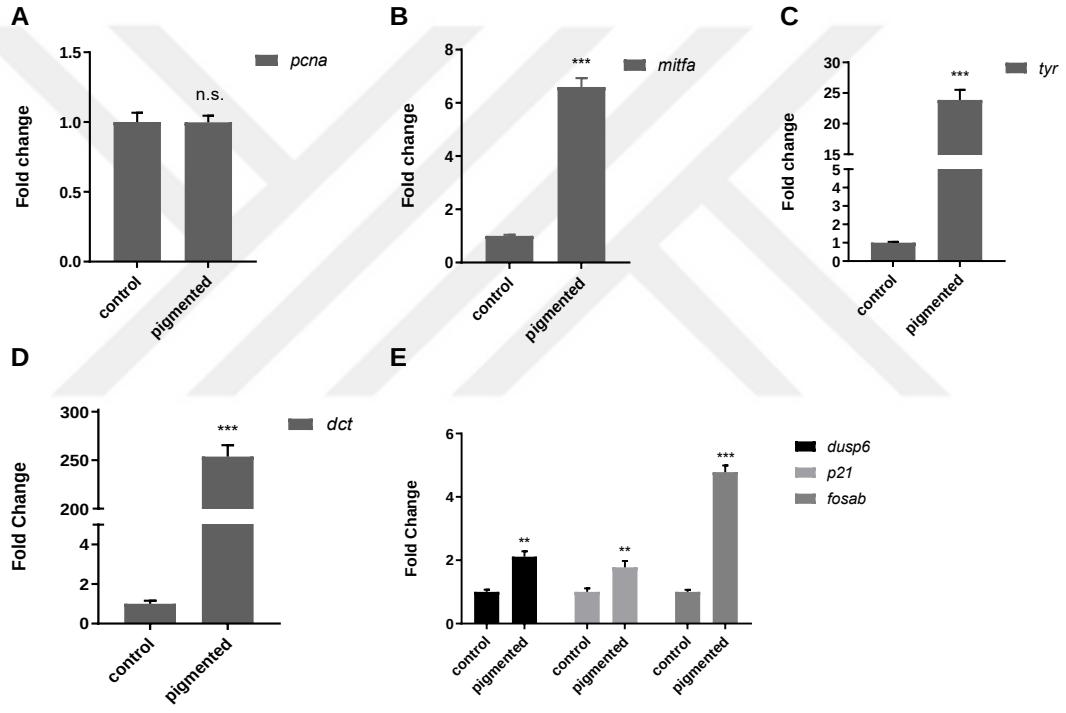

Figure 3.10 Real-time PCR analysis of mRNAs of *pcna, mitfa, tyr, dct, dusp6, p21* and *fosab* for the control and hyper-pigmented tumor developed on caudal fin. *rpl13* was used as endogenous control. Relative mRNA level was normalized to the corresponding *rpl13* mRNA expression. qPCR data presented here are means ± SD from triplicate data. Asterisk on individual bars represents significant difference between control group and NCP groups. Student's t test was used to calculate significance *P < 0.05, **P < 0.01 (Student's unpaired ttest). Error bars indicate SEM. Data represented here compares the expression levels of **(A)** *pcna* between control and the pigmented melanoma (p= 0,9971) **(B)** *mitfa* between control between control and the tumor (p= <0,0001) **(C)** *tyr* between control between control and the tumor (p= <0,000) (**D)** *dct* between control between control and the tumor (p= <0,0001). **(E)** *dct* between control between control and the tumor (*dusp6* p= 0,0002, *p21* p= 0,0002, *fosab* p= <0,0001).

The melanoma developed on anal fin was hypo-pigmented. Same in cauda fin, we excised tumor, took anal fin as control and checked for melanocyte regeneration markers and for the markers mostly altered in melanoma transformation. We found that expression of melanocyte regeneration markers (*dct* and *tryp1*) were low compared to control group. The increase in the expression of altered pathways of *dusp6* (RAS target), *p21* (pI3K/AKT target) and *fosab* (Erk/MAPK target) was higher in hypo-pigmented melanoma when compared to hyper-pigmented tumor (Fig.310). The fold changes for hyper-pigmented melanoma nearly 2-fold for both *dusp6* and *p21*; 5-fold for *fosab*. On the other hand, hypo-pigmented melanoma bears much more increased expression of *dusp6*, *p21* and *fosab*; 30, 100 and 80-fold increase, respectively (Figure 3.11).

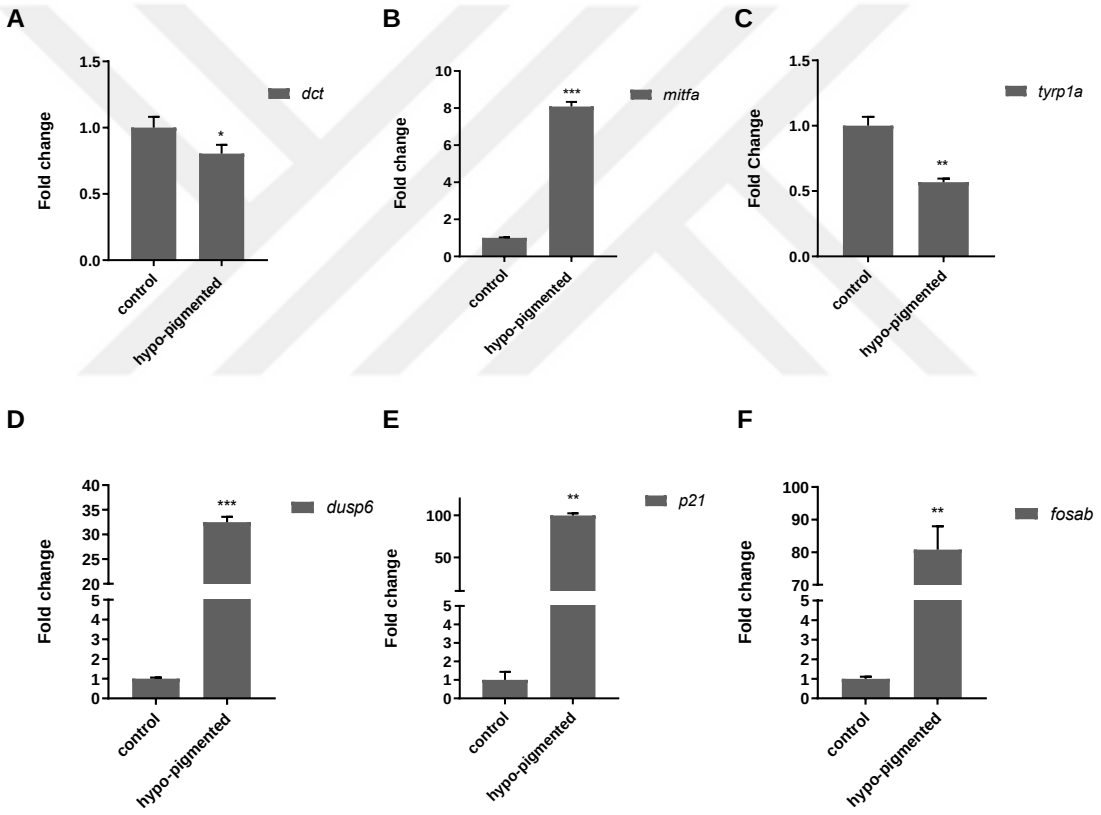

Figure 3.11 Real-time PCR analysis of mRNAs of *mitfa*, *dct* and *tyrp1* for the control and hypo-pigmented tumor developed on anal fin. *rpl13* was used as endogenous control. Relative mRNA level was normalized to the corresponding *rpl13* mRNA expression. qPCR data presented here are means ± SD from triplicate data. Asterisk on individual bars represents significant difference between control group and NCP groups. Student's t test was used to calculate significance *P < 0.05, **P < 0.01 ***P < 0.001 (Student's unpaired ttest). Error bars indicate SEM. Data represented here compares the expression levels of **(A)** *mitf* between control and the tumor (p= 0,0125). **(B)** *dct* between control between control and the tumor (p= <0,0001). **(C)** *tyrp1a* between control between control and the tumor (p= <0,0001). **(D)** *dusp6* between control and the tumor (p= <0,0001). **(E)** *p21* between control between control and the tumor (p= 0,0084). **(F)** *fosab* between control between control and the tumor (p= 0,0010).

Next, we checked neural crest markers on hypo-pigmented melanoma since it showed de-differentiated character according to qPCR analysis. We found that the expression of *crestin*, *dlx2a*, *sox10* and *mitf* markers related to neural crest identity had higher expression in melanoma than control.

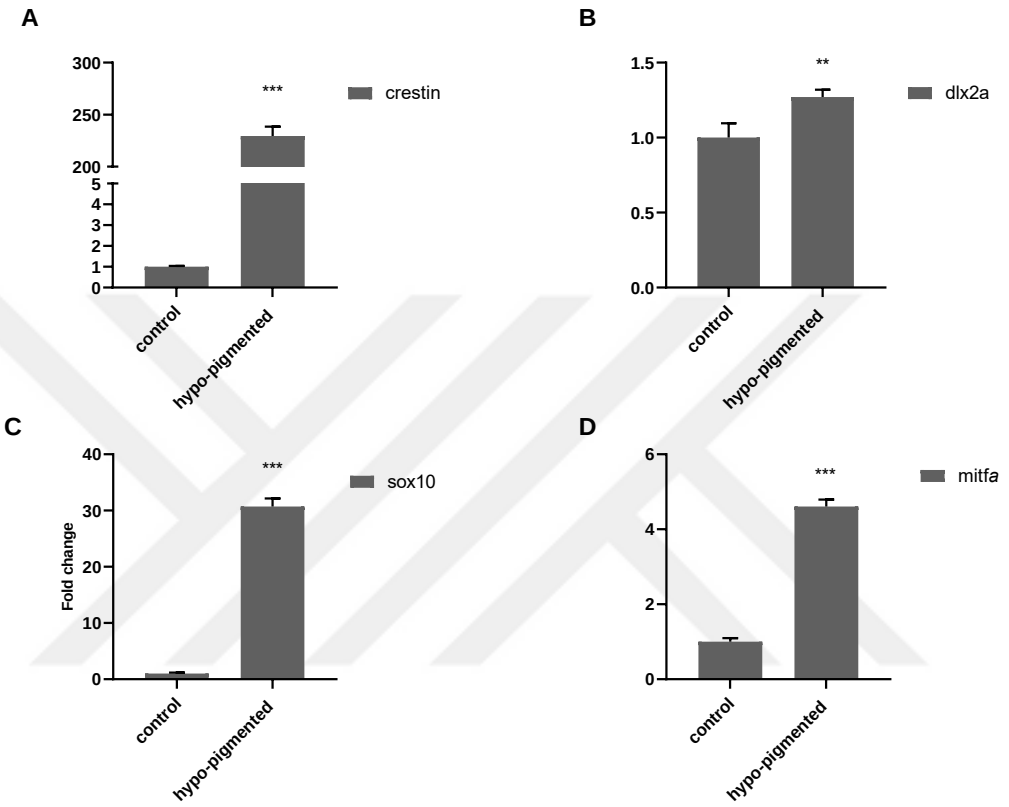

Figure 3.12 Real-time PCR analysis of mRNAs for *crestin*, *dlx2a*, *sox10* and *mitf* for the control and hypo-pigmented tumor developed on anal fin. *rpl13* was used as endogenous control. Relative mRNA level was normalized to the corresponding *rpl13* mRNA expression. qPCR data presented here are means ± SD from triplicate data. Asterisk on individual bars represents significant difference between control group and NCP groups. Student's t test was used to calculate significance *P < 0.05, **P < 0.01, ***P < 0.001 (Student's unpaired ttest). Error bars indicate SEM. Data represented here compares the expression levels of **(A)** *crestin* between control and the tumor (p= <0,0001). **(B)** *dlx2a* between control between control and the tumor (p= 0,009). **(C)** *sox10* between control between control and the tumor (p= <0,0001). **(D)** *mitf* between control between control and the tumor (p= <0,0001).

DISCUSSION

Determination of early and late stages of melanocyte regeneration constitutes the basis of our study since we will build future studies on these results. We applied NCP based ablation to kill all melanocyte of fish. The first cumulative loss of melanocyte aggregates appeared on the body at 3 dpa. Even though melanocyte aggregates are not extruded out of the fin, they totally lost their dendritic morphologies and displayed a smear of scattered black aggregates. In this stage we can say that melanocytes lost all their cellular activities. We found that at 4 dpa most of the melanocytes are disposed out of skin and pigmentation started to appear all over the body at 7 dpa and the pigment pattern is accomplished until 15 dpa (C. Yang et al., 2006).

The action mechanism of NCP was not revealed completely so far. However, previous studies showed that NCP-induced melanocyte death was inhibited by exogenous $CuCl_2$ indicating that NCP may have a role as copper chelator in melanocyte ablation (O'Reilly-Pol & Johnson, 2008). Melanocytes are sensitive to copper depletion because an important differentiation enzyme *tyr* requires copper as a co-factor to be functional. NCP based melanocyte ablation is specific when compared to other ablation methods. In fin resection regeneration model, whole cells start to regenerate to restore the amputated fin. On the other hand, the exact distinction of early and late stages of regeneration would not be possible since rounds of proliferation and differentiation events are overlapped in blastema mediated regeneration. Laser is also widely used to ablate melanocytes. However, in this technique there is possibility of destroying other pigments (Akyilmaz, Yorganci, & Asav, 2010, pp. 8–10; O'Reilly-Pol & Johnson, 2008).

We wanted to assure that all or at least most of melanocytes on the fin are dead after 24 hours of NCP treatment. Therefore, we treated control and NCP treated fish with epinephrine at 1 dpa and 2 dpa. Epinephrine treatments showed that melanocyte did not respond at 1 dpa and 2 dpa whereas melanocytes of untreated fish respond within 15-20 minutes by losing dendritic shapes and turning into compacted rounds. However, the response of melanocytes to epinephrine is not reconstructing the cell shape. Instead, melanin containing melanosomes aggregates towards the nucleus in the existence of epinephrine signal. Epinephrine binds Gi coupled receptors and decrease cAMP level in cytoplasm. cAMP in melanocytes has role in melanosome travel along microtubules and transfer to actin filaments (Iyengar et al., 2015; Sheets, Ransom, Mellgren, Johnson, & Schnapp, 2007). The melanocytes at 1 dpa and 2 dpa

were unable to respond to epinephrine because they were dead. This result shows that one-day treatment of NCP induced melanocyte ablation was successful.

We chose the markers used in qPCR to determine early and late stages of regeneration based on literature. m*itf* is the master regulator of melanocyte development. It is active at very early stages of melanocyte development/regeneration, even before the differentiation process begin. *mitf* is required to establish melanoblast fate and then to activate the mechanism that leads melanocyte differentiation. (Ceol et al., 2008). Our qPCR results that compare the expression of *mitf* showed that *mitf* expression was higher in 4 dpa when compared to control. The expression level was decreased at 7 dpa. This indicates that early melanocyte regeneration proceeds to 4 dpa. The importance of *mitf* in development reflect its importance in melanocyte regeneration because the molecular pathways are similar in both processes. Even though *mitf* expression is high in early stages to provide survival and proliferation of developing and regenerating melanocytes, the expression does not cease totally in later stages. At late stages of regeneration *mitf* act as transcriptional factor of differentiation markers such as *tyr*, *dct* and *tryp1*(Rawls, Mellgren, & Johnson, 2001). *mitf* keeps its activity throughout the melanocyte existence. Having found that differentiation markers were higher at 4 dpa than control led us to take consider that early proliferative state of melanocyte regeneration should be before 4 dpa. And from the literature we knew that proliferative activities begin at 1 dpa in adult melanocyte regeneration and diminish after 4 dpa (Iyengar et al., 2015). Therefore, we checked *pcna* expression at 1, 2, 3, 4 and 7 dpa. After 1 dpa, we observed gradual decrease in *pcna* expression. The decrease continued untill *pcna* expression is balanced with the control group at 7 dpa. Therefore, we determined 1 dpa as early stage of melanocyte regeneration in which expression of differentiation markers were not yet detected. To determine the late stage of melanocyte regeneration we analyzed the expression of melanocyte differentiation markers*; dct, tyr, tyrp1a* and *tyrp1b* by qPCR. We found that differentiation markers had the highest expression at 7 dpa when pigmentation starts all over the body and determined 7 dpa as late melanocyte regeneration stage.

Here we used an established melanoma model of zebrafish (*kita*:HRAS^{G12V}:GFP). This model provides RAS oncogene dependent melanoma transformation in which HRAS^{G12V} under the kita promoter led melanocyte hyperproliferation and melanoma growth. kit receptor is involved in the commitment of melanoblast lineage and migration of melanocyte precursors to the proper sites and *kit* is continuously active in melanocyte lineage (Gilbert, 2014, p. 382).

HRAS overexpression led melanoma growth in 2 months without the need of additional inactivating mutations on tumor suppressor. *mitfa*+/-; *kita*:HRAS^{G12V}:GFP fish carry mutated version of HRAS in which at the 12th position glycine is replaced with the valine amino acid. This substitution lead permanent activation of HRAS protein that drives cells to grow in uncontrolled manner (Forbes et al., 2017).

We found that 17% of 2-month-old fish and 36% of 5-month-old fish developed melanoma. HRAS^{G12V} mutation alone under *kita* promoter to induce hyperproliferation was enough to induce melanoma. Ectopic melanocytic spots started to accumulate beginning from 3 days post fertilization and within a few weeks' benign lesions developed during early embryogenesis. We observed melanocytic hyperplasia and melanoma growth on the body, fins and tail. We had the advantage of using HRAS^{G12V} oncogene under kita promoter because kita expressing melanoblast population concentrated on the fin where we modelled our regeneration experiments. The other advantage of RAS induced melanoma in zebrafish is that it represents similar histopathology to human melanoma (Dovey, White, & Zon, 2009; Michailidou et al., 2009; Santoriello et al., 2010).

Melanoma is determined by a various histopathological characteristic. We examined the sections and ask several questions to characterize the nature of the melanoma developed on fish. Does melanoma have distinct borders, or display growth that disrupt the borders? Are cells invasive? Did they distort the microanatomical structures? What is the morphology of the melanoma cells and the degree of nuclear polymorphism (Detrich, Zon, & Westerfield, 2017, pp. 352–353)? In this study, histological evaluation showed that *kita*:HRAS^{G12V}:GFP melanoma had vertical growth pattern and invasive characteristics to various tissues and organs beside benign lesions (horizontal growth). We can say that benign lesions on *kita*:HRAS^{G12V}:GFP fish is similar to superficial spreading melanoma (SSM) that has brown-black coloration with irregular borders (Šitum, Buljan, Kolić, & Vučić, 2014). Vertical growth, infiltrations, degenerations on muscle bundles, spindle/epithelioid shaped cells and marks of mild nuclear polymorphism led us to come to an end that melanoma is malignant. However, a histopathologist that has practice in routine diagnostic should investigate the specimens to determine the degree of malignancy. For this, we need to make counting for mitotic figures to determine rate of the melanoma proliferation. On the other hand, we haven't observed high degree of spindle shaped cells; melanoma in this study is mostly composed of epithelioid shaped cells. Besides, we observed low number of melanophages indicating melanoma could have

progressed malignancy. Even though epithelioid shaped cells in tumor is the sign of more aggressive malignant neoplasm we haven't observed nuclear polymorphism (variation in the size and shape of the cell/cell nuclei). Nevertheless, the melanoma pathology has diverse characteristics which differs by a combination of architectural and cytological features (Detrich et al., 2017, pp. 352–353). Therefore, we need to perform further histopathological studies such as IHC to confirm the nature of melanoma induced in *kita*:HRAS^{G12V}:GFP line.

We showed that hypo-pigmented melanoma acquired neural crest identity according to qPCR analysis. The expression of *crestin, dlx2a, sox10* and *mitf* markers which are related to neural crest identity were analyzed and found that all have higher expression in melanoma than control. Expression of *crestin* which is a neural crest progenitor in zebrafish is lost after 72 hours post fertilization. However, *crestin* instantly is re-expresed in malignant transformation of melanoma which could be exploited as a tracker for malignant onset. *crestin* function has not been revealed yet it shows similar expression pattern on zebrafish embryo with *sox10* which a neural crest progenitor marker (Kaufman et al., 2016). Besides, we found that *mitf* expression is higher in hypo-pigmented and hyper-pigmented melanoma. There has been two proposal for the *mitf* level in melanoma; the first that *mitf* abrogation is related to melanoma regression and the second *mitf* amplification is related to poor prognosis. However, we know that there are different subtypes of melanoma in which all of them do not show the similar genetic background. On one hand *mitf* is required for differentiation genes to be activated in the melanocyte fate, on the other hand *mitf* is required for proliferation and survival. In melanoma, *mitf* probably mostly is active for melanoma cells to survive and proliferate rather than differentiate (Kim et al., 2017; Lister et al., 2014).

In our studies zebrafish as a model organism provided numerous advantages. We took the advantage of modeling melanocyte regeneration and melanoma within the same organism to reveal the common and different aspects of both processes. Previous studies conducted on zebrafish melanocyte biology provided insight into the nature of melanocyte regeneration. These studies contributed us to determine proliferative and differentiation stages of melanocyte regeneration. We easily performed melanocyte ablation and regeneration follow-up due to black melanin content of melanocytes. We could track day by day melanocyte death, disposal and regeneration. We also had the advantage of exploiting established transgenic line to generate our melanoma models. Zebrafish is an excellent model to use different melanocyte specific promoter to drive various oncogenes and promote melanoma growth in either spatially

and temporally control manner. Besides, many tumor suppressors and oncogenes are conserved between zebrafish and human. In our histopathological examinations, RAS induced melanomas provided easy characterization of zebrafish melanoma due to similar histopathology to human melanoma. We will be able to easily distinguish the benign and malignant stages of zebrafish melanoma by using human melanoma markers to make further characterization (Detrich et al., 2017, pp. 340–342).

CONCLUSION

We showed that melanocyte regeneration and melanoma can be modelled on zebrafish caudal fin. Both contexts can be successfully compared within the same organism on the same organ. Even at 3 dpf larva, we observed melanocyte hyperproliferation indicating that melanocyte growth leads melanoma transformation at adulthood. Besides, continuous activation of HRAS under *kita* promoter would enable us to track benign lesions transformations to malignant melanoma. Therefore, we demonstrated that already used zebrafish melanoma model is convenient tool to compare the early and late melanocyte regeneration profiles to benign and malignant melanoma in our studies. Early and late melanocyte regeneration clearly displays difference in the expression levels of differentiation markers. Hyper-pigmented and hypo-pigmented melanoma displays difference in the late melanocyte regeneration markers, which indicates that hypo-pigmented melanoma loses all their differentiated states and acquire neural crest cell identity.

PERSPECTIVES

Once we established melanocyte regeneration and melanoma models of zebrafish, we will analyze differentially expressed genes in both two distinct cellular contexts by deep transcriptome profiling. Additionally, we will retrieve gene expression profiles of human skin cutaneous melanoma to compare with the regenerating zebrafish melanocyte and different stages of melanoma. We will aim to reveal whether melanocyte regeneration and melanoma transcriptome profile follow common or distinct route at early and late stages. Then, we will generate zebrafish melanoma cell line from an established zebrafish melanoma model, or we will receive an established zebrafish melanoma cell line to test whether cancer cell can be directed to regeneration phase where cells are switched to differentiation state from dedifferentiation state and uncontrolled proliferation is stopped. We will choose genes that are significantly altered in melanocyte regeneration and melanoma to perform knock-out/knock-in experiment in zebrafish melanoma cell line in order to practice transplantation/xenograft studies of these modified melanoma cell lines. Therefore, we will be able to observe how these modifications influence melanoma progression such as proliferation, metastasis and angiogenesis.

REFERENCES

Akyilmaz, E., Yorganci, E., & Asav, E. (2010). Do copper ions activate tyrosinase enzyme? A biosensor model for the solution. *Bioelectrochemistry*, *78*(2), 155–160. https://doi.org/10.1016/j.bioelechem.2009.09.007

Alberts, B., Johnson, A., Lewis, J., Raff, M., Roberts, K., & Walter, P. (2002). *Molecular Biology of the Cell*. https://doi.org/10.1017/CBO9781107415324.004

Amatruda, J. F., & Patton, E. E. (2008). Chapter 1 Genetic Models of Cancer in Zebrafish. *International Review of Cell and Molecular Biology*, *271*(C), 1–34. https://doi.org/10.1016/S1937-6448(08)01201-X

Arunachalam, M., Raja, M., Vijayakumar, C., Malaiammal, P., & Mayden, R. L. (2013). Natural History of Zebrafish (*Danio rerio*) in India. *Zebrafish*, *10*(1), 1–14. https://doi.org/10.1089/zeb.2012.0803

Bergman, W., & Gruis, N. A. (2010). Management of melanoma families. *Cancers*, *2*(2), 549–566. https://doi.org/10.3390/cancers2020549

Betters, E., Liu, Y., Kjaeldgaard, A., Sundström, E., & García-Castro, M. I. (2010). Analysis of early human neural crest development. *Developmental Biology*, *344*(2), 578–592. https://doi.org/10.1016/j.ydbio.2010.05.012

Bevona, C., Goggins, W., Quinn, T., Fullerton, J., Tsao, H., & Corona, R. (2003). Cutaneous Melanomas Associated with Nevi. *Archives of Dermatology*, *139*(12), 1620–1624. https://doi.org/10.1001/archderm.139.12.1620

Bhowmick, N. A., Neilson, E. G., & Moses, H. L. (2004). and progression, *432*(November).

Carlson, B. M. (2007). Principles of Regenerative Biology. *Principles of Regenerative Biology*, 259–278. https://doi.org/10.1016/B978-0-12-369439-3.X5000-4

Carpio Y., & Estrada. (2002). Zebrafish as a genetic model organism. *Biotecnologia Aplicada*, *2006*(10), 23(4).

Ceol, C. J., Houvras, Y., White, R. M., & Zon, L. I. (2008). Melanoma Biology and the Promise of Zebrafish. *Zebrafish*, *5*(4), 247–255. https://doi.org/10.1089/zeb.2008.0544

Chávez, M. N., Aedo, G., Fierro, F. A., Allende, M. L., & Egaña, J. T. (2016). Zebrafish as an emerging model organism to study angiogenesis in development and regeneration. *Frontiers in Physiology*, *7*(MAR). https://doi.org/10.3389/fphys.2016.00056

Cichorek, M., Wachulska, M., Stasiewicz, A., & Tymi??ska, A. (2013). Skin melanocytes:

Biology and development. *Postepy Dermatologii i Alergologii*, *30*(1), 30–41. https://doi.org/10.5114/pdia.2013.33376

Clark, W. H., Elder, D. E., Guerry, D., Epstein, M. N., Greene, M. H., & Van Horn, M. (1984). A study of tumor progression: The precursor lesions of superficial spreading and nodular melanoma. *Human Pathology*, *15*(12), 1147–1165. https://doi.org/10.1016/S0046-8177(84)80310-X

Crusz, S. M., & Balkwill, F. R. (2015). Inflammation and cancer: Advances and new agents. *Nature Reviews Clinical Oncology*, *12*(10), 584–596. https://doi.org/10.1038/nrclinonc.2015.105

Davies, H., Bignell, G. R., Cox, C., Stephens, P., Edkins, S., Clegg, S., … Futreal, P. A. (2002). 6-Mutations of the BRAF gene in human cancer. *Nature*, *417*(6892), 949–954. https://doi.org/10.1038/nature00766

Detrich, H. W., Zon, L. I., & Westerfield, M. (2017). *The zebrafish : disease models and chemical screens*. *Methods in cell biology* (Vol. 138). https://doi.org/10.1016/B978-0-12-381320-6.00010-2

Dipietro, L. A. (2013). Angiogenesis and scar formation in healing wounds. *Current Opinion in Rheumatology*, *25*(1), 87–91. https://doi.org/10.1097/BOR.0b013e32835b13b6

Dolberg, D. S., Hollingsworth, R., Hertle, M., & Bissell, M. J. (1985). Wounding and its role in RSV-mediated tumor formation. *Science*, *230*(4726), 676–678. https://doi.org/10.1126/science.2996144

Dovey, M., White, R. M., & Zon, L. I. (2009). Oncogenic NRAS Cooperates with *p53* Loss to Generate Melanoma in Zebrafish. *Zebrafish*, *6*(4), 397–404. https://doi.org/10.1089/zeb.2009.0606

Dunham, L. J. (1972). Cancer in Man at Site of Prior Benign Lesion of Skin or Mucous Membrane: A Review. *Cancer Research*, *32*(7), 1359–1374.

Dupin, E., & Le Douarin, N. M. (2003). Development of melanocyte precursors from the vertebrate neural crest. *Oncogene*, *22*(20), 3016–3023. https://doi.org/10.1038/sj.onc.1206460

Dvorak, H. F. (1986). Tumors: wounds that do not heal. Similarities between tumor stroma generation and wound healing. *The New England Journal of Medicine*, *315*(26), 1650–1659. https://doi.org/10.1056/NEJM198612253152606

Erickson, C. A., & Reedy, M. V. (1998). 5 Neural Crest Development: The Interplay between

Morphogenesis and Cell Differentiation. *Current Topics in Developmental Biology, 40*, 177–209. https://doi.org/10.1016/S0070-2153(08)60367-1

Ernfors, P. (2010). Cellular origin and developmental mechanisms during the formation of skin melanocytes. *Experimental Cell Research*, *316*(8), 1397–1407. https://doi.org/10.1016/j.yexcr.2010.02.042

Ferrara, N., & Kerbel, R. S. (2005). Angiogenesis as a therapeutic target. *Nature*, *438*(7070), 967–974. https://doi.org/10.1038/nature04483

Fitzpatrick, T. B. (1961). The Reciprocal Relationship between Melanization and Tyrosinase Activity in Melanosom . es (Melanin Granules) In mammals , melanin pigment is synthesized in a specific cell , the melanocyte , by the action of a copper-containing oxidase , into a large, *49*(6).

Forbes, S. A., Beare, D., Boutselakis, H., Bamford, S., Bindal, N., Tate, J., … Campbell, P. J. (2017). COSMIC: somatic cancer genetics at high-resolution. *Nucleic Acids Research*, *45*(D1), D777–D783. https://doi.org/10.1093/nar/gkw1121

Fountain, J. W., Karayiorgou, M., Ernstoff, M. S., Kirkwood, J. M., Vlock, D. R., Titus-Ernstoff, L., … Lahti, J. (1992). Homozygous deletions within human chromosome band 9p21 in melanoma. *Proceedings of the National Academy of Sciences of the United States of America*, *89*(November), 10557–10561. https://doi.org/10.1073/pnas.89.21.10557

Friedmann-Morvinski, D., Bushong, E. A., Ke, E., Soda, Y., Marumoto, T., Singer, O., … Verma, I. M. (2012). Dedifferentiation of neurons and astrocytes by oncogenes can induce gliomas in mice. *Science*, *338*(6110), 1080–1084. https://doi.org/10.1126/science.1226929

Garbe, C., Peris, K., Hauschild, A., Saiag, P., Middleton, M., Bastholt, L., … Eggermont, A. M. (2016). Diagnosis and treatment of melanoma. European consensus-based interdisciplinary guideline - Update 2016. *European Journal of Cancer*, *63*, 201–217. https://doi.org/10.1016/j.ejca.2016.05.005

Gilbert, S. F. (2014). Developmental Biology. *Book*, 719.

Goessling, W., & North, T. E. (2014). Repairing quite swimmingly: advances in regenerative medicine using zebrafish. *Disease Models & Mechanisms*, *7*(7), 769–776. https://doi.org/10.1242/dmm.016352

Grose, R. (2002). A crucial role of [beta] 1 integrins for keratinocyte migration in vitro and during cutaneous wound repair. *Development*, *129*, 2303–2315.

Gruber, F., Ka, M., Brajac, I., Safti, M., & Peharda, V. (2008). Molecular and Genetic Mechanisms in Melanoma. *Collegium Antropologicum*, *32*(November), 147–152.

Haddow, A. (1973). Molecular repair, wound healing, and carcinogenesis: Tumor production a possible overhealing? *Advances in Cancer Research*, *16*(C), 181–234. https://doi.org/10.1016/S0065-230X(08)60341-3

Hanahan, D., & Weinberg, R. A. (2000). The Hallmarks of Cancer Review University of California at San Francisco, *100*, 57–70.

Hanahan, D., & Weinberg, R. A. (2011). Review Hallmarks of Cancer : The Next Generation. *Cell*, *144*(5), 646–674. https://doi.org/10.1016/j.cell.2011.02.013

Hearing, V. J. (2011). Determination of Melanin Synthetic Pathways. *Journal of Investigative Dermatology*, *131*, E8–E11. https://doi.org/10.1038/skinbio.2011.4

Holly, E. A., Kelly, J. W., Shpall, S. N., & Chiu, S.-H. (1987). Number of melanocytic nevi as a major risk factor for malignant melanoma. *J Am Acad Dermatol*, *17*(3), 459–468. https://doi.org/10.1016/S0190-9622(87)70230-8

Holstein, T. W., & David, A. (1991). of Epithelial. *Developmental Biology*, *611*, 602–611.

Iyengar, S., Kasheta, M., & Ceol, C. J. (2015). Poised Regeneration of Zebrafish Melanocytes Involves Direct Differentiation and Concurrent Replenishment of Tissue-Resident Progenitor Cells. *Developmental Cell*, *33*(6), 631–643. https://doi.org/10.1016/j.devcel.2015.04.025

Jopling, C., Boue, S., & Belmonte, J. C. I. (2011). Dedifferentiation, transdifferentiation and reprogramming: Three routes to regeneration. *Nature Reviews Molecular Cell Biology*, *12*(2), 79–89. https://doi.org/10.1038/nrm3043

Karin, M., & Clevers, H. (2016). Reparative inflammation takes charge of tissue regeneration. *Nature*, *529*(7586), 307–315. https://doi.org/10.1038/nature17039

Karlsson, J., von Hofsten, J., & Olsson, P.-E. (2001). Generating Transparent Zebrafish: A Refined Method to Improve Detection of Gene Expression During Embryonic Development. *Marine Biotechnology*, *3*(6), 0522–0527. https://doi.org/10.1007/s1012601-0053-4

Kawakami, K. (2007). Tol2: A versatile gene transfer vector in vertebrates. *Genome Biology*, *8*(SUPPL. 1), 1–10. https://doi.org/10.1186/gb-2007-8-s1-s7

Kim, I. S., Heilmann, S., Kansler, E. R., Zhang, Y., Zimmer, M., Ratnakumar, K., … White, R. M. (2017). Microenvironment-derived factors driving metastatic plasticity in melanoma.

Nature Communications, *8*(May 2016), 1–11. https://doi.org/10.1038/ncomms14343

Lister, J. A., Capper, A., Zeng, Z., Mathers, M. E., Richardson, J., Paranthaman, K., … Patton, E. E. (2014). A conditional zebrafish MITF mutation reveals MITF levels are critical for melanoma promotion vs. regression in vivo. *Journal of Investigative Dermatology*, *134*(1), 133–140. https://doi.org/10.1038/jid.2013.293

Lush, M. E., & Piotrowski, T. (2014). Sensory hair cell regeneration in the zebrafish lateral line. *Developmental Dynamics*, *243*(10), 1187–1202. https://doi.org/10.1002/dvdy.24167

Mani, S. A., Guo, W., Liao, M. J., Eaton, E. N., Ayyanan, A., Zhou, A. Y., … Weinberg, R. A. (2008). The Epithelial-Mesenchymal Transition Generates Cells with Properties of Stem Cells. *Cell*, *133*(4), 704–715. https://doi.org/10.1016/j.cell.2008.03.027

McCampbell, K. K., & Wingert, R. A. (2014). New tides: Using zebrafish to study renal regeneration. *Translational Research*, *163*(2), 109–122. https://doi.org/10.1016/j.trsl.2013.10.003

Michailidou, C., Jones, M., Walker, P., Kamarashev, J., Kelly, A., & Hurlstone, A. F. L. (2009). Dissecting the roles of Raf- and PI3K-signalling pathways in melanoma formation and progression in a zebrafish model. *Disease Models & Mechanisms*, *2*(7–8), 399–411. https://doi.org/10.1242/dmm.001149

Morgan, T. H. (1898). Experimental studies of the regeneration of Planaria maculata. *Archiv f??R Entwickelungsmechanik Der Organismen*, *7*(2–3), 364–397. https://doi.org/10.1007/BF02161491

Neurosurg, J., Zool, J. E., & Neurol, J. C. (2007). PRINCIPLES OF REGENERATIVE BIOLOGY Copyright © 2007 by Academic Press. Inc. All rights of reproduction in any form reserved. 325, 12846–12851.

O'Reilly-Pol, T., & Johnson, S. L. (2008). Neocuproine ablates melanocytes in adult zebrafish. *Zebrafish*, *5*(4), 257–264. https://doi.org/10.1089/zeb.2008.0540

Paavonen, K., Puolakkainen, P., Jussila, L., Jahkola, T., & Alitalo, K. (2000). Vascular endothelial growth factor receptor-3 in lymphangiogenesis in wound healing. *American Journal of Pathology*, *156*(5), 1499–1504. https://doi.org/10.1016/S0002-9440(10)65021-3

Park, H. D., Ortmeyer, A. B., & Blankenbaker, D. P. (1970). Cell division during regeneration in hydra. *Nature*, *227*(5258), 617–619. https://doi.org/10.1038/227617a0

Plonka, P. M., Passeron, T., Brenner, M., Tobin, D. J., Shibahara, S., Thomas, A., …

Schallreuter, K. U. (2009). What are melanocytes really doing all day long...? *Experimental Dermatology*, *18*(9), 799–819. https://doi.org/10.1111/j.1600-0625.2009.00912.x

Poss, K. D. (2010). Advances in understanding tissue regenerative capacity and mechanisms in animals. *Nature Reviews Genetics*, *11*(10), 710–722. https://doi.org/10.1038/nrg2879

Price, A. C., Weadick, C. J., Shim, J., Rodd, F. H., & Al, P. E. T. (2008). Pigments , Patterns , and Fish Behavior, *5*(4).

Rabbani, P., Takeo, M., Chou, W., Myung, P., Bosenberg, M., Chin, L., … Ito, M. (2011). Coordinated activation of wnt in epithelial and melanocyte stem cells initiates pigmented hair regeneration. *Cell*, *145*(6), 941–955. https://doi.org/10.1016/j.cell.2011.05.004

Rawls, J. F., & Johnson, S. L. (2000). Zebrafish kit mutation reveals primary and secondary regulation of melanocyte development during fin stripe regeneration, *3724*, 3715–3724.

Rawls, J. F., Mellgren, E. M., & Johnson, S. L. (2001). How the zebrafish gets its stripes. *Developmental Biology*, *240*(2), 301–314. https://doi.org/10.1006/dbio.2001.0418

Riss, J., Khanna, C., Koo, S., Chandramouli, G. V. R., Yang, H. H., Hu, Y., … Barrett, J. C. (2006). Cancers as wounds that do not heal: Differences and similarities between renal regeneration/repair and renal cell carcinoma. *Cancer Research*, *66*(14), 7216–7224. https://doi.org/10.1158/0008-5472.CAN-06-0040

Sánchez Alvarado, A. (2000). Regeneration in the metazoans: Why does it happen? *BioEssays*, *22*(6), 578–590. https://doi.org/10.1002/(SICI)1521-1878(200006)22:6<578::AID-BIES11>3.0.CO;2-#

Santoriello, C., Gennaro, E., Anelli, V., Distel, M., Kelly, A., Köster, R. W., … Mione, M. (2010). Kita driven expression of oncogenic HRAS leads to early onset and highly penetrant melanoma in zebrafish. *PLoS ONE*, *5*(12), 1–11. https://doi.org/10.1371/journal.pone.0015170

Schäfer, M., & Werner, S. (2008). Cancer as an overhealing wound: An old hypothesis revisited. *Nature Reviews Molecular Cell Biology*, *9*(8), 628–638. https://doi.org/10.1038/nrm2455

Schmidt, E. E., Ichimura, K., Messerle, K. R., Goike, H. M., & Collins, V. P. (1997). Infrequent methylation of CDKN2A(MTS1/p16) and rare mutation of both CDKN2A and CDKN2B(MTS2/p15) in primary astrocytic tumours. *British Journal of Cancer*, *75*(1), 2–8. https://doi.org/10.1038/bjc.1997.2

Sebolt-Leopold, J. S., & Herrera, R. (2004). Targeting the mitogen-activated protein kinase cascade to treat cancer. *Nature Reviews Cancer*, *4*(12), 937–947. https://doi.org/10.1038/nrc1503

Serrano, M., Hannon, G. J., & Beach, D. (1993). A new regulatory motif in cell-cycle control causing specific inhibition of cyclin D/CDK4. *Nature*, *366*(6456), 704–707. https://doi.org/10.1038/366704a0

Seuradge, J., & Wong, E. (2019). Melanoma | McMaster Pathophysiology Review. Retrieved from http://www.pathophys.org/melanoma/

Sheets, L., Ransom, D. G., Mellgren, E. M., Johnson, S. L., & Schnapp, B. J. (2007). Zebrafish Melanophilin Facilitates Melanosome Dispersion by Regulating Dynein. *Current Biology*, *17*(20), 1721–1734. https://doi.org/10.1016/j.cub.2007.09.028

Shoji, W., & Sato-Maeda, M. (2008). Application of heat shock promoter in transgenic zebrafish. *Development Growth and Differentiation*, *50*(6), 401–406. https://doi.org/10.1111/j.1440-169X.2008.01038.x

Siebert, S., Anton-Erxleben, F., & Bosch, T. C. G. (2008). Cell type complexity in the basal metazoan Hydra is maintained by both stem cell based mechanisms and transdifferentiation. *Developmental Biology*, *313*(1), 13–24. https://doi.org/10.1016/j.ydbio.2007.09.007

Šitum, M., Buljan, M., Kolić, M., & Vučić, M. (2014). Melanoma - Clinical, dermatoscopical, and histopathological morphological characteristics. *Acta Dermatovenerologica Croatica*, *22*(1), 1–12.

Spence, R., Gerlach, G., Lawrence, C., & Smith, C. (2008). The behaviour and ecology of the zebrafish, Danio rerio. *Biological Reviews*, *83*(1), 13–34. https://doi.org/10.1111/j.1469-185X.2007.00030.x

Sugumaran, M. (1991). Molecular mechanisms for mammalian melanogenesis. Comparison with insect cuticular sclerotization. *FEBS Lett*, *295*(1–3), 233–239. https://doi.org/10.1016/0014-5793(91)81140-4

Sulaimon, S. S., & Kitchell, B. E. (2003). Review article the biology of melanocytes. *Veterinary Dermatology*, *14*(2), 57–65. https://doi.org/10.1046/j.1365-3164.2003.00327.x

Tal, T. L., Franzosa, J. A., & Tanguay, R. L. (2010). Molecular signaling networks that choreograph epimorphic fin regeneration in Zebrafish - A mini-review. *Gerontology*, *56*(2), 231–240. https://doi.org/10.1159/000259327

Tanaka, E. M., & Reddien, P. W. (2011). The Cellular Basis for Animal Regeneration. *Developmental Cell*, *21*(1), 172–185. https://doi.org/10.1016/j.devcel.2011.06.016

Tse, J. C., & Kalluri, R. (2007). Mechanisms of metastasis: Epithelial-to-mesenchymal transition and contribution of tumor microenvironment. *Journal of Cellular Biochemistry*, *101*(4), 816–829. https://doi.org/10.1002/jcb.21215

TSONIS, P. A., & EGUCHI, G. (1982). Abnormal Limb Regeneration without Tumor Production in Adult Newts Directed by Carcinogens, 20-Methylcholanthrene and Benzo (α) pyrene: amphibia/limb regeneration/carcinogen/teratogenesis. *Development, Growth & Differentiation*, *24*(2), 183–190. https://doi.org/10.1111/j.1440-169X.1982.00183.x

Urasaki, A., Asakawa, K., & Kawakami, K. (2008). Efficient transposition of the Tol2 transposable element from a single-copy donor in zebrafish. *Proceedings of the National Academy of Sciences*, *105*(50), 19827–19832. https://doi.org/10.1073/pnas.0810380105

Visvader, J. E. (2011). Cells of origin in cancer. *Nature*, *469*(7330), 314–322. https://doi.org/10.1038/nature09781

Waddington, C. H. (1935). Cancer and the theory of organisers. *Nature*, *135*(3416), 606–608. https://doi.org/10.1038/135606a0

White, R. M., & Zon, L. I. (2008). Melanocytes in Development, Regeneration, and Cancer. *Cell Stem Cell*, *3*(3), 242–252. https://doi.org/10.1016/j.stem.2008.08.005

Whiteman, D. C., Green, A. C., & Olsen, C. M. (2016). The Growing Burden of Invasive Melanoma: Projections of Incidence Rates and Numbers of New Cases in Six Susceptible Populations through 2031. *Journal of Investigative Dermatology*, *136*(6), 1161–1171. https://doi.org/10.1016/j.jid.2016.01.035

Yang, C., Johnson, S. L., Yang, C., & Johnson, S. L. (2006). Small molecule-induced ablation and subsequent regeneration of larval zebrafish melanocytes. *Development*, *133*(22), 4607–4607. https://doi.org/10.1242/dev.02692

Yang, C. T., Sengelmann, R. D., & Johnson, S. L. (2004). Larval melanocyte regeneration following laser ablation in zebrafish. *Journal of Investigative Dermatology*, *123*(5), 924–929. https://doi.org/10.1111/j.0022-202X.2004.23475.x

Zhao, S., Huang, J., & Ye, J. (2015). A fresh look at zebrafish from the perspective of cancer research. *Journal of Experimental and Clinical Cancer Research*, *34*(1), 1–9. https://doi.org/10.1186/s13046-015-0196-8

APPENDIX

Ethical committee approval

T.C.
DOKUZ EYLÜL ÜNİVERSİTESİ
İZMİR ULUSLARARASI BİYOTIP VE GENOM ENSTİTÜSÜ
HAYVAN DENEYLERİ YEREL ETİK KURULU (İBG-HADYEK)
KARARI

İBG-Enstitü

TOPLANTI TARİHİ	17/05/2017	TOPLANTI GÜNÜ	Çarşamba
TOPLANTI SAYISI	08	TOPLANTI SAATİ	15.00

Sayın Doç.Dr. H.Güneş ÖZHAN,

13/2016 Protokol No'lu; yürütücüsü olduğunuz "Comparison of the molecular mechanisms of melanocyte regeneration and melanoma using the zebrafish" başlıklı projenin uygulanmasında etik açıdan sakınca olmadığına oy birliği ile karar verilmiştir.

Bilgilerinizi ve gereğini rica ederiz.

Prof.Dr. Ensari GÜNELİ **Başkan**	**Prof.Dr. H. Alper BAĞRIYANIK** **Başkan Yardımcısı**
Prof. Dr. Belgin ÜNAL **Üye** **(KATILAMAMIŞTIR)**	**Doç.Dr. Ralph Meuwissen** **Üye**
Doç.Dr. Devrim PESEN OKVUR **Üye**	**Doç.Dr. H. Güneş ÖZHAN** **Üye** **(PROJE YÜRÜTÜCÜSÜ)**
Uzm. Kerem ESMEN **Üye**	**Uzm. Umur KELEŞ** **Üye**
Ecz. Ferdane KAHRAMAN **Üye** **(KATILAMAMIŞTIR)**	